EUMETSAT ECMWF

EUMETSAT/ECMWF Fellowship Programme Research Report

50

Investigations into the assimilation of AMSU-A in the presence of cloud and precipitation

P. Weston, A. Geer, N. Bormann

September 2019

Series: EUMETSAT/ECMWF Fellowship Programme Research Reports

A full list of ECMWF Publications can be found on our web site under:
http://www.ecmwf.int/en/publications/

Contact: library@ecmwf.int

European Centre for Medium Range Weather Forecasts, Shinfield Park, Reading, RG2 9AX, UK

Abstract

The all-sky assimilation of AMSU-A radiances has been investigated and compared to the clear-sky approach currently used operationally. This work is motivated by the aim to assimilate all microwave instruments through the all-sky system in the future. With this in mind, a detailed investigation of differences in the assimilation configurations between the separate clear-sky and all-sky assimilation systems has been performed. The majority of these differences have been addressed with the all-sky configuration now sharing many common settings with the clear-sky configuration. This is motivated by the fact that the AMSU-A clear-sky configuration has been fine-tuned and optimised over many years so improving upon it with different settings would be difficult.

The experimentation shows that the all-sky assimilation of AMSU-A now replicates the large forecast impact of the clear-sky assimilation in the extra-tropics, while allowing up to 20% more observations to be assimilated for the lowest AMSU-A sounding channels. There are small but significant improvements to short-range forecasts of temperature, humidity and wind in the extra-tropics, while medium-range forecasts are generally neutral. However, short-range temperature, humidity and wind forecasts in the tropics are slightly degraded.

A number of possible future enhancements to the AMSU-A all-sky configuration have been identified which will hopefully lead to improved results and, along with the progress made so far, should enable the all-sky assimilation of AMSU-A and other microwave temperature sounding instruments to become operational in the future.

1 Introduction

This paper reports on the development of the all-sky assimilation of Advanced Microwave Sounding Unit - A (AMSU-A) radiances at the European Centre for Medium-range Weather Forecasts (ECMWF). This is compared against the existing clear-sky assimilation where cloud-affected radiances are screened out and not assimilated. Many issues related to differences between the all-sky and clear-sky assimilation methodologies have been addressed and remaining issues are also documented.

Microwave temperature sounding radiances, primarily from AMSU-A, have been assimilated into global numerical weather prediction (NWP) models for the last 20 years and have consistently provided significant positive impacts on forecast accuracy. This is due to the global coverage available from satellite-based instruments, the microwave temperature sounding instruments' observation errors being dominated by well-characterised instrument noise, and weaker sensitivity to cloud and precipitation than infrared radiances. However, AMSU-A channels sensitive in the lowest part of the atmosphere do have non-negligible sensitivity to cloud and precipitation. Until recently, AMSU-A radiances from these channels have only been assimilated after cloud- and precipitation-affected radiances have been screened out.

In recent years ECMWF has developed the all-sky assimilation of microwave imagers and humidity sounders with significant positive impacts on medium-range forecasts (Geer et al., 2017). The main benefits come from the 4D-Var tracing effect (Peubey and McNally, 2009) where misplaced cloud and precipitation features in the forecasts are corrected by adjusting the wind-field at different times throughout the 4D-Var assimilation window. The development and good performance of all-sky assimilation has relied on important improvements to the all-sky observation operator (RTTOV-SCATT) (Geer and Baordo, 2014) and has also led to the discovery of biases caused by inaccuracies in the model cloud parameterisations (Lonitz and Geer, 2015).

There are three main motivating factors for moving AMSU-A to all-sky assimilation. Firstly, two separate systems for assimilating satellite radiances have been developed at ECMWF: one to assimilate radiances in clear skies, where any cloud-affected observations are rejected; and one to assimilate ra-

diances in all cloud and precipitation conditions. It would simplify the overall assimilation system and reduce maintenance if all microwave instruments could be assimilated through the all-sky system and the clear-sky system became redundant. Secondly, given recent advances in all-sky assimilation of other microwave instruments as mentioned above, it is hoped that forecast improvements can be achieved with AMSU-A and other current and future microwave temperature sounding instruments (e.g. ATMS, MWTS, MWS) when assimilated in all-sky. Finally, AMSU-A channel 4 (52.8GHz) is not currently assimilated in the clear-sky system because of its significant cloud sensitivity. Moving to all-sky assimilation allows the additional assimilation of channel 4 to be tested with potential for further forecast improvements.

The all-sky assimilation of temperature-sounding channels is more challenging than the humidity-sounding channels. This is because the temperature background errors to be corrected are much smaller than the humidity background errors. Also microwave temperature-sounding observations have a much more non-linear response to cloud and precipitation than humidity-sounding observations. For example, for AMSU-A channel 5 (53.6GHz), the presence of cloud liquid water has a positive effect on the radiances due to increased emission, but frozen hydrometeors generally have a negative effect due to increased scattering (Geer et al., 2012).

An initial aim of this work is to replicate the present operational AMSU-A impact in the all-sky system. The present clear-sky assimilation of AMSU-A has been fine-tuned over almost 20 years, and this aspect adds to the general challenge of assimilating temperature-sounding channels in cloud and precipitation-affected regions. Once a comparable impact is achieved it is hoped that enhancements specific to all-sky assimilation can be made to improve the results. This follows the strategy used to develop the all-sky assimilation of the the microwave imagers and humidity sounding channels at ECMWF where initial results were neutral before incremental enhancements have steadily improved the impact in recent years (Geer et al., 2017).

Previous work to assimilate AMSU-A in cloud and precipitation at ECMWF (Geer et al., 2012) yielded mixed results and interpretation of those results was hindered by a number of fundamental differences in how the observations are treated in the two separate systems. Since ECMWF model cycle 43r1 it has been possible to mimic the clear-sky assimilation of observations through the all-sky system. This enables the impacts of the technical differences between the two systems to be isolated from the impacts coming from the additional assimilation of radiances in the presence of cloud and precipitation. Much of section 2 and appendix A are dedicated to understanding, removing (where possible) and quantifying the impact of the differences between the clear-sky treatment of observations in the clear- and all-sky systems.

There has been recent progress in this area both at NCEP (Zhu et al., 2016) and the Met Office (Migliorini and Candy, 2019). Both schemes use a similar approach to the all-sky methodology developed at ECMWF with a variable observation error which results in assigning larger observation errors in cloudy areas (Geer and Bauer, 2011). They found considerable benefits in short and medium-range forecast scores. However, neither of these systems assimilate any other observation types in all-sky conditions and precipitation-affected observations are explicitly screened out in the all-sky treatment.

The paper is structured as follows: the technical differences between the clear- and all-sky systems and all-sky configuration details are addressed in section 2; details of the experiments are included in section 3; experiment results are presented in section 4; and conclusions are drawn and ideas of future developments are summarised in section 5. Further details on the differences between the clear- and all-sky systems are included in appendix A.

2 All-sky and clear-sky assimilation at ECMWF

There are two separate systems and code paths which are used to pre-process and assimilate radiances at ECMWF. The first is the clear-sky assimilation system where a clear-sky radiative transfer model (RTTOV, Saunders et al. (2018)) is used within the observation operator and observations affected by cloud and precipitation are screened out prior to the assimilation. This system is presently used operationally to assimilate AMSU-A, ATMS and MWHS observations at ECMWF. The second is the all-sky assimilation system where observations are assimilated in clear, cloudy, and precipitating conditions. A radiative transfer model (RTTOV-SCATT) is used, which takes model cloud fields as an input to simulate cloud and precipitation effects in the radiances, such as cloud liquid water emission and ice scattering. This system is presently used operationally to assimilate microwave humidity-sounding and imaging channels from MHS, MWHS-2, SSMIS, SAPHIR, GMI and AMSR-2.

In this paper, moving AMSU-A from the clear-sky assimilation system into the all-sky assimilation system is investigated. There are several subtle differences between the assimilation choices in the two systems which make it difficult to directly compare assimilating AMSU-A in the clear-sky system against assimilating AMSU-A in the all-sky system. These differences are scientifically motivated, for example in the clear-sky system observations which are most likely to be cloud-free are chosen within the thinning procedure, which does not make sense in the all-sky system. In order to allow a more informative comparison an intermediate clear-sky-through-all-sky (CLEAR-ALL) configuration is run. This is where the all-sky assimilation system is used to assimilate the AMSU-A radiances but the clear-sky radiative transfer and simplified cloud screening procedures are used to mimic the clear-sky usage of the data. This configuration is not fully optimised as it is never planned to become operational but it should allow the impact coming from the technical differences between the two systems to be isolated from the impact of the additional assimilation of the cloud- and precipitation-affected AMSU-A data.

Table 1 summarises the configurations of the different systems and some of these aspects are further discussed below and in appendix A. In order to make the comparison between the clear-sky assimilation of AMSU-A radiances in the all-sky system and the clear-sky system as fair as possible a number of fundamental differences between the two systems had to be addressed. Some initial differences which were eliminated in the final configuration included inconsistent quality control procedures and the horizontal interpolation method. The clear-sky configuration was replicated in the all-sky system for these aspects which were simply technical choices and had small impacts on forecast performance, details of which can be found in appendices A.1 and A.2. Making these changes resulted in improved short-range forecasts of temperature and smaller AMSU-A first guess departures.

2.1 Cloud detection

The cloud detection in the CLEAR system aims to identify cloud-affected observations, and the current operational scheme is described by Lawrence et al. (2015). It uses a combination of checks on window channel departures, retrieved liquid water path (LWP) and a scattering index (SI) which are summarised in Tab. 2. The liquid water path retrieval (Grody et al., 2001) uses brightness temperatures from channels 1 (23.8GHz) and 2 (31.4GHz). The scattering index is simply the difference in brightness temperatures between channels 1 and 15 (89.0GHz) (Bennartz et al., 2002).

The cloud detection in the CLEAR system has been designed together with an observation error model which takes account of the effects of residual unmodelled clouds. For the CLEAR-ALL approach, the full complexity of the operational cloud detection is not replicated. Instead, a simplified version is used, with

Aspect	Clear-sky (CLEAR)	Clear-sky-through-all-sky (CLEAR-ALL)	All-sky (ALL)
Radiative transfer	RTTOV (clear-sky)	RTTOV (clear-sky)	RTTOV-SCATT (all-sky)
Cloud detection (see also Tab. 2)	Full	Simplified	None
Observation errors	Noise, cloud and surface dependent	Noise dependent	Noise and cloud dependent
Thinning	125x125km boxes	T_L255 reduced Gaussian grid	T_L255 reduced Gaussian grid
Skin temperature sink variable	Yes	No	No
Quality control	Basic, first guess check and VarQC	As CLEAR plus some all-sky specific checks	As CLEAR-ALL
Bias correction	VarBC with constant, air mass and third order polynomial scan predictors	As CLEAR	As CLEAR
Interpolation	Bi-linear/bi-cubic	As CLEAR with nearest neighbour for cloud hydrometeors and land-sea mask	As CLEAR-ALL
Surface emissivity	Over ocean: FASTEM emissivity model. Over land: dynamic emissivity retrieval using channel 3 (50.3GHz) radiances without bias correction	As CLEAR	As CLEAR

Table 1: Summary of the assimilation configuration for the clear-sky, clear-sky-through-all-sky and all-sky systems. Details of each of the aspects are explained throughout section 2

CLEAR			
Ocean		Land & sea ice	
Channel(s)	Check	Channel(s)	Check
5	$\|O-B\|_{50.3GHz} > 3$K	5-8	$\|O-B\|_{52.8GHz} > 0.7$K
6-8	SI > 5K	5,6	SI > 3K
5,6	LWP > 0.3kg/m^2		
CLEAR-ALL			
Ocean		Land & sea ice	
Channel(s)	Check	Channel(s)	Check
5-8	$\|O-B\|_{50.3GHz} > 3$K	5-8	$\|O-B\|_{52.8GHz} > 0.7$K

Table 2: Summary of cloud detection checks used in CLEAR and CLEAR-ALL. N.B. any checks affecting channel 8 are only applied in the tropics ($|\text{latitude}| < 30$)

a single cloud check over each surface type as detailed in Tab. 2. This decision was based on a thorough analysis of the numbers of observations rejected by each of the cloud detection checks. Over ocean, the most important check is the channel 3 first guess departure check with the other checks affecting many fewer observations. Therefore, this check was kept but extended to channels 6 and 7 (and 8 in the tropics) which results in a small reduction in the number of observations assimilated from channels 5 to 7 in the CLEAR-ALL compared to the CLEAR configuration. This is one of the few remaining differences between these two configurations which it is important to note when interpreting results in section 4.2.

The window channel departure checks also screen out observations in areas where there are few clouds but which suffer from surface-related biases such as over the Sahara desert. The check hence protects the analysis and forecasts from these surface-related biases being aliased into atmospheric increments (Bormann et al., 2017).

2.2 Observation error model

Observation errors are modelled very differently in the CLEAR and ALL systems, reflecting the different error characteristics of the assimilated data (Geer and Bauer, 2011). In the CLEAR system Lawrence et al. (2015) introduced a situation-dependent observation error model including noise, cloud and surface dependent terms with strict thresholds on how large the observation error could become. In the CLEAR-ALL configuration the observation error is fixed using a similar value to the noise term in the CLEAR observation error model with some inflation for channels 5 and 6 to attempt to match the average observation error from the clear-sky error model. In the ALL system the assumed observation error aims to model the larger representation errors in cloud-affected regions (Geer and Bauer, 2011). It therefore varies as a function of symmetric cloud amount, the mean of the predicted cloud from the model and observations as described further below. Table 3 gives example values for the CLEAR, CLEAR-ALL and ALL error models for MetOp-B AMSU-A.

The all-sky error model requires a reliable cloud predictor at the same locations as the observations to be assimilated. Over ocean, the retrieved liquid water path from both observations and model simulations is used as the cloud predictor (Grody et al., 2001). Over land, the 23GHz - 89GHz scattering index is used as the cloud predictor. This cloud predictor is predominantly sensitive to frozen hydrometeors due to enhanced scattering at 89GHz compared to 23GHz.

The all-sky observation error model is derived by binning the standard deviation of first guess departures by the value of the symmetric cloud predictors for each channel, following Geer and Bauer (2011). Figure 1 shows that the AMSU-A channel 5 first guess departures vary quadratically with retrieved cloud liquid water over ocean. As expected the standard deviation of first guess departures increase with increasing cloud amount until they plateau. The green line shows the observation error model (fitted by eye) used for this channel which closely matches the shape of the standard deviation of first guess departures. Similarly, Fig. 2 shows that the AMSU-A channel 6 (54.4GHz) first guess departures vary quadratically with 23-89GHz scattering index over land. Again, the green line shows the observation error model which follows the standard deviation of first guess departures. A quadratic model is suitable for channels 5 to 8 over land and channels 5 and 6 over ocean. A linear model is used for channels 7 (54.94GHz) and 8 (55.5GHz) over ocean. In addition, it was found that there is even a small variation in the standard deviation of first guess departures for channel 9 (57.29GHz) so this channel also uses a situation dependent error with a very small linear increase between clear and cloudy errors. This channel's peak sensitivity is around 90hPa so it is perhaps sensitive to some of the highest convective clouds in the tropics which justifies the use of a cloud-dependent error for this channel.

	CLEAR	CLEAR-ALL	ALL	
Channel	Noise term	Clear	Clear	Cloudy
5	0.27	0.3	0.27	2.5
6	0.18	0.19	0.18	0.7
7	0.19	0.19	0.18	0.27
8	0.2	0.2	0.19	0.21
9	0.19	0.19	0.19	0.22
10	0.24	0.24	0.25	0.25
11	0.34	0.34	0.34	0.34
12	0.5	0.5	0.5	0.5
13	0.84	0.84	0.84	0.84
14	1.4	1.4	1.4	1.4

Table 3: Assigned observation errors (K) for the CLEAR, CLEAR-ALL and ALL error models for MetOp-B AMSU-A over ocean. The CLEAR errors shown in the table are just from the noise term and do not include the surface or cloud terms of the Lawrence et al. (2015) error model

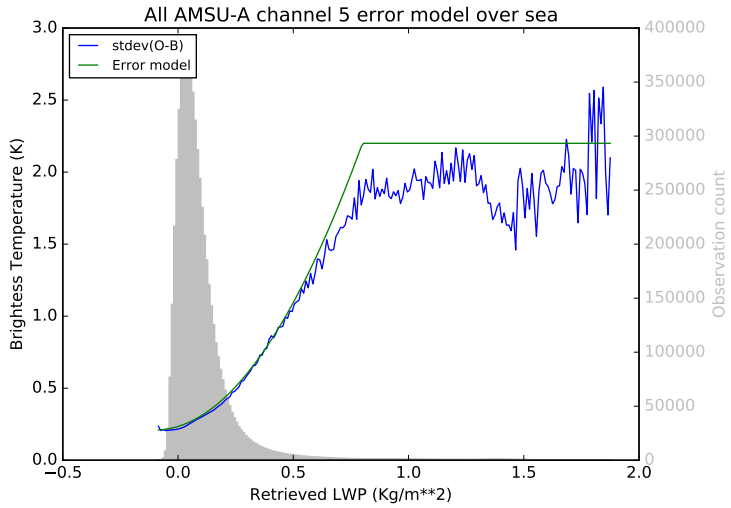

Figure 1: Variability of the standard deviation of first guess departures with retrieved cloud liquid water for AMSU-A channel 5 over ocean

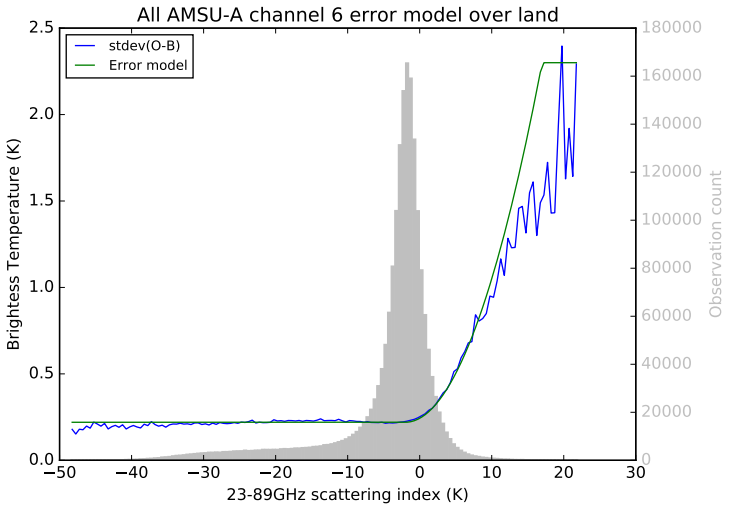

Figure 2: Variability of the standard deviation of first guess departures with 23-89GHz scattering index for AMSU-A channel 6 over land

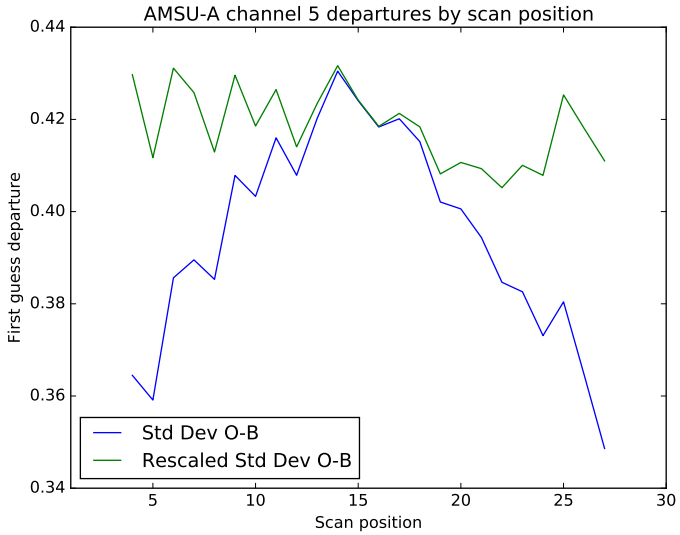

Figure 3: Variability of the standard deviation of first guess departures with scan position for NOAA-19 AMSU-A channel 5

An additional scan dependent observation error term was used by Geer et al. (2012) to account for variability across the scan caused by enhanced sensitivity to clouds and the surface at nadir compared to the edge of the scan. This same model:

$$f(\theta) = 0.3 + 0.7exp(-\frac{(\beta\theta)^2}{2}) \quad (1)$$

is used here, where θ is the satellite zenith angle and β is a tunable parameter which has been re-computed and is now 1.4 for channel 3, 1.7 for channel 4 and 0.9 for channel 5. Figure 3 shows that the standard deviation of first guess departures are larger near the centre than at the edge of the scan for channel 5 and that rescaling by dividing by $f(\theta)$ removes this variability. An exponential function is used due to the Gaussian shape of the observation error variability with scan position.

For some satellites the AMSU-A channels used to compute the cloud predictors are missing or broken. In this case the assimilation configuration reverts to CLEAR-ALL where cloud detection and clear-sky radiative transfer are used. This is currently the case for MetOp-B AMSU-A over land (due to broken channel 15) and Aqua AMSU-A over ocean and land (due to broken channels 1 and 2).

2.3 Thinning

Thinning is used to reduce the effects of spatially correlated observation errors which are not accounted for directly. In the clear-sky system the globe is split up into 125x125km thinning boxes and, for each instrument, only one observation can be used in each of these boxes, per 30 minutes. For instruments that are present on multiple satellites, such as AMSU-A, this procedure treats all observations from different satellites together. This means that in areas where the satellite tracks overlap, such as at high latitudes, only one AMSU-A observation will be used in each thinning box. When there are multiple available observations in a thinning box the observation to be used is the one which has the smallest window channel first guess departure. This is effectively an additional form of cloud detection as observations with smaller window channel first guess departures are more likely to be in cloud-free areas.

The thinning procedures are quite different in the all-sky system. Firstly, there is no window channel departure check used in the all-sky system because cloud detection procedures are not required. Instead, the observations are chosen based on their distance from alternate points of a T_L255 reduced Gaussian grid. Effectively this is equivalent to using $\sim$110x110km thinning boxes. In isolation, this should result in significantly more AMSU-A observations being used in the all-sky system compared to the clear-sky system. However, there is an extra check in the all-sky system where an observation is not used if it lies more than 30km away from the nearest T_L255 reduced Gaussian grid point. This distance threshold has been tuned to ensure that the overall number of observations assimilated in non-cloud-affected channels is very similar between the clear- and all-sky systems. Despite this tuning, the different thinning methods result in a slightly different distribution of assimilated observations, with fewer observations used at high zenith angles and more observations used at nadir in the ALL system as shown in Fig. 4. This is because, at high zenith angles, the effective field of view (FOV) size is larger and the FOVs are further apart meaning that more observations are discarded by the 30km distance threshold check in the all-sky system. For near-nadir positions, the spatial sampling in the all-sky system is therefore more dense than in the clear-sky system, and the all-sky system is potentially more exposed to neglected spatially correlated observation errors. In contrast, sampling is less dense in regions covered by outer scan-positions.

In both systems, all of the AMSU-A instruments on different satellites are thinned together. This was not the case in some of the initial experimentation where the different satellites were thinned separately

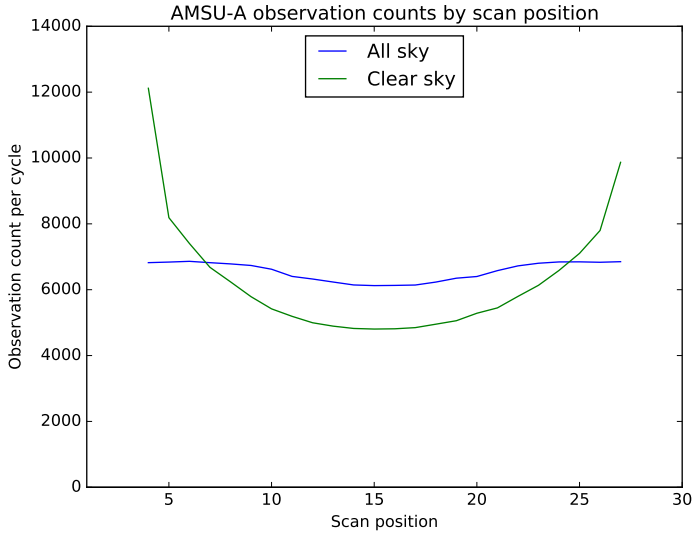

Figure 4: Number of AMSU-A observations assimilated per assimilation window in clear-sky (green) and all-sky (blue) systems binned by scan position. AMSU-A observations from the 3 scan positions closest to each edge of the scan are not assimilated due to large residual biases

in the all-sky system. Results from these experiments revealed that these thinning choices do make quite a large difference to the accuracy of short-range forecasts with significantly improved fits to independent observations, more details can be seen in appendix A.3.

2.4 Surface-sensitive channels

The use of surface-sensitive channels such as AMSU-A channel 5 requires accurate skin temperature and surface emissivity values for the radiative transfer calculations. In the clear-sky system over ocean, the surface emissivity is calculated using the FASTEM emissivity model (Liu et al., 2011), and this is also adopted in the all-sky system[1]. Over land, it is dynamically retrieved using AMSU-A channel 3 radiances before bias correction (Karbou et al., 2006). A similar methodology is used in the all-sky system (Baordo and Geer, 2016) although, for all other all-sky observation types, bias corrected radiances are used in the emissivity retrieval. This choice was made by Baordo and Geer (2016) to primarily correct for instrument specific biases affecting SSMIS. AMSU-A does not suffer from this type of bias to the same extent and using the radiances without bias correction in the emissivity retrieval resulted in an improvement to the short-range temperature forecasts which can be seen in appendix A.4. Therefore, the AMSU-A radiances used in the emissivity retrieval are not bias corrected in the experiments introduced in section 3.

The clear-sky system uses a so-called sink variable for the skin temperature. This means skin temperature is retrieved from the assimilated observations at each field of view during 4D-Var, using the model

[1]The FASTEM emissivity and reflectivity are intended for radiances (i.e. they are valid at a specified zenith angle) and they are "effective" since they are adjusted for non-specular reflection using an estimate of the clear-sky surface to space transmittance. The all-sky approach using RTTOV-SCATT makes use of FASTEM as well. However, the cloudy surface to space transmittance is used in the calculation of effective emissivity and reflectivity for the cloudy column. Further, although the surface boundary conditions in the scattering solver require estimates of hemispheric (flux) emissivity and reflectivity, the assumption is made that the FASTEM effective emissivities can be used. This may cause small differences between clear-sky and all-sky simulations (and is also the case for all other all-sky sensors).

(a)

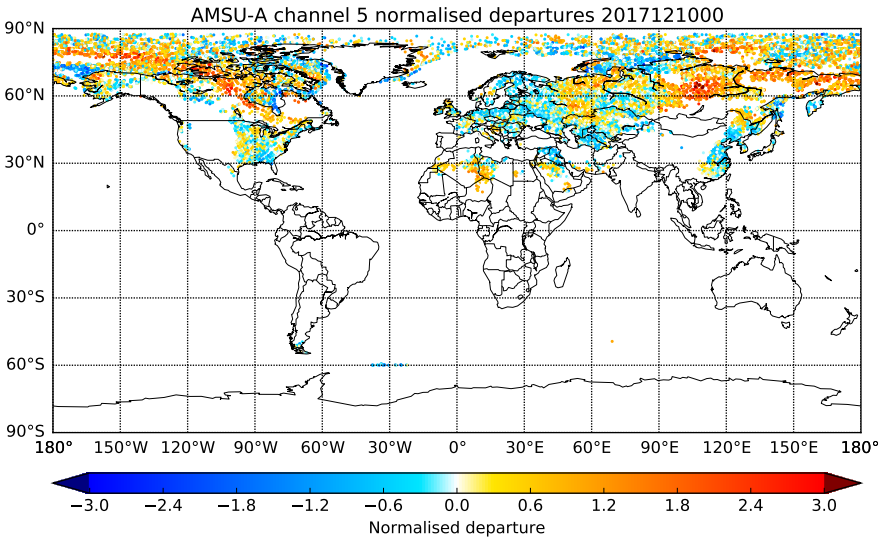

(b)

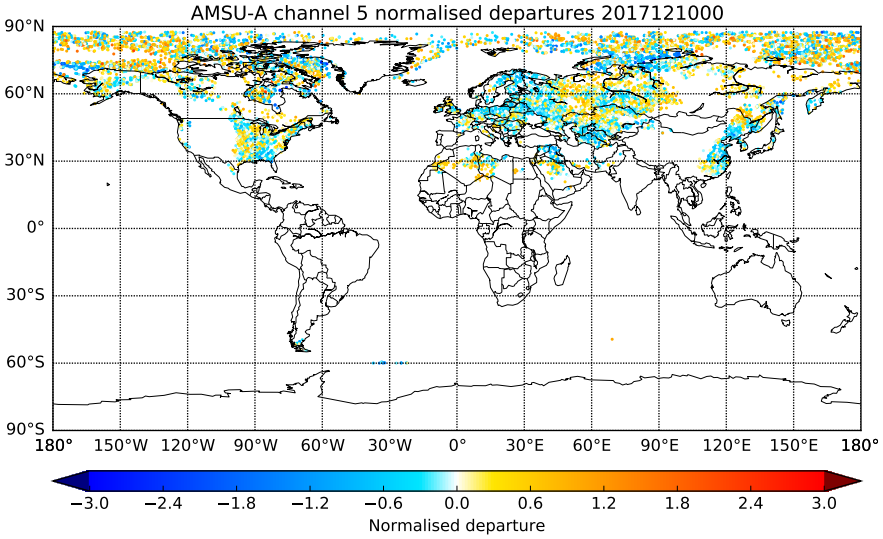

Figure 5: Maps of AMSU-A channel 5 first guess departures after bias correction divided by observation error (a) before additional channel 4 first guess departure check (b) after additional channel 4 first guess departure check. The sample plotted are observations over surfaces classified as snow (land surface temperature <278K) and sea ice (model sea ice >0.01 or sea surface temperature <273.15K)

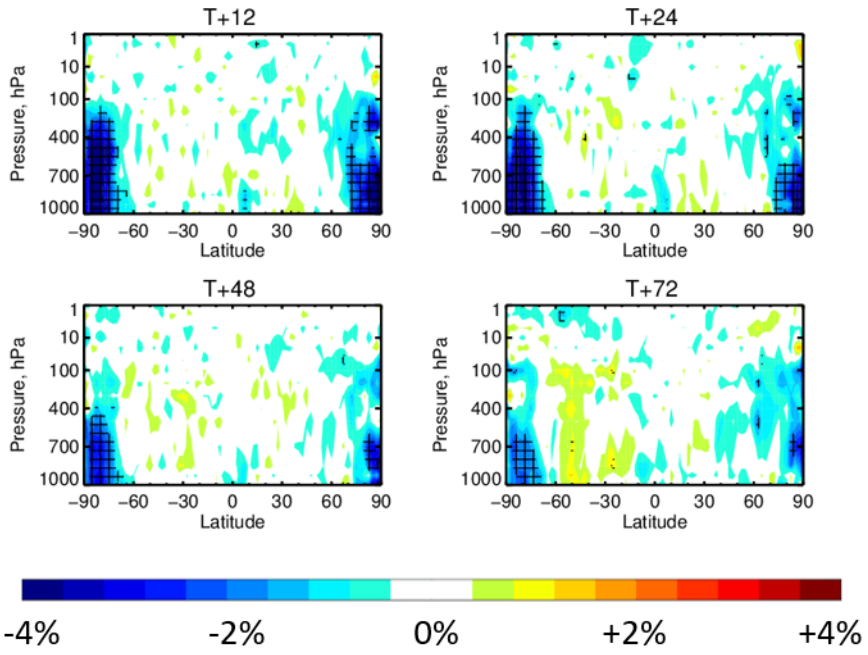

Figure 6: Latitude-pressure plot of the change in temperature forecast RMSE at T+12, 24, 48 and 72 hours when including additional quality control for AMSU-A all-sky over snow and sea ice. Experiments were run for a total of 6 months.

values as background. Separate values are retrieved for each field of view (without taking into account spatial or temporal background error correlations for the skin temperature), and the retrieved values are subsequently discarded after the minimisation. The main purpose of this is to reduce the effect of random errors in the background skin temperature for surface-sensitive channels. It also helps to protect against other surface-related biases, such as those from inaccurate surface emissivity, being aliased into atmospheric increments.

The skin temperature sink variable is not used in the all-sky system with the justification that cloud effects in the first guess departures could incorrectly be aliased into skin temperature increments. This means there is less protection against surface-related biases affecting the atmospheric analysis in the all-sky system.

Initial experimentation showed that there were large areas of significant residual biases in AMSU-A channel 5 over snow and sea ice regions, see Fig. 5a, which were causing degradations to short-range temperature forecasts. This bias is also present in the clear-sky system but very few observations are assimilated in these areas. This is due to a combination of the skin temperature sink variable, emissivity term in the clear-sky observation error model and the cloud screening.

In areas of snow and sea ice there are a couple of possible reasons for biases. Firstly, the radiative transfer model assumes specular reflection of radiation whereas in snowy areas there could be some Lambertian reflection too which could lead to residual biases (Bormann et al., 2017). Secondly, microwave radiation is able to penetrate deep into certain types of snow such as very dry snow. Currently the snow model is a single layer which is not able to represent the temperature profile within the snow pack. A multi-layer snow model is under development which may help to improve the biases over this area.

A pragmatic solution to this is to reinstate the clear-sky quality control check on the channel 4 departures just over snow and sea ice in the all-sky system. The same bias affects channels 4 and 5 so this check successfully removes the worst affected observations, see Fig. 5b. This check may not be perfect as it will also potentially be screening out cloud-affected radiances in these areas but it does result in significant improvements of up to 4% in temperature forecast scores at high latitudes, see Fig. 6. The ALL experiment outlined in section 3 uses this channel 4 departure check over snow and sea ice.

Another potential solution to this problem is to use the channel 4 departure as an alternative to the scattering index as the cloud predictor in the error model over land. This would then down-weight data in areas with the biases seen above as well as accounting for cloud liquid water which the scattering index is not as sensitive to. This will be the subject of future research.

2.5 Quality control

Quality control is used to prevent the assimilation of poor quality observations and also observations whose values cannot be simulated accurately enough in the radiative transfer model. Table 4 summarises the percentage of AMSU-A channel 5 observations which fail the various quality control checks in the clear- and all-sky systems. Some of these checks are relaxed for the higher peaking channels.

More observations are screened out due to cloud in CLEAR-ALL compared to CLEAR due to the simplified cloud detection introduced in section 2.1. Far fewer observations are cloud screened in ALL but some still are due to the broken window channel 15 on MetOp-B AMSU-A which means MetOp-B AMSU-A channels 5-8 revert to having cloud detection applied over land only. The first guess departure check results in slightly more rejections in CLEAR-ALL which is due to the lack of an error model resulting in generally smaller observation errors and hence tighter quality control. Variational quality control (VarQC, Anderson and Järvinen (1999)) is used to reject observations which are likely to have gross errors not picked up by the other checks. The use of VarQC has played an important role in the sucess of the all-sky assimilation of the MW imagers and humidity sounding channels (Geer and Bauer, 2011). It is interesting to see a slight increase in the number of AMSU-A observations rejected through VarQC in ALL compared to CLEAR and CLEAR-ALL despite the parameters being kept constant.

2.6 Bias correction

The approach to bias correction used in the present study for the clear-sky and the all-sky assimilation of AMSU-A is the same. In both cases variational bias correction (Dee, 2004; Auligné et al., 2007) is used, as is done for the vast majority of radiances in the ECMWF system. The bias models are also the same, and for most channels they use a constant term along with four air mass predictors in a linear model, with a third-order polynomial in the scan-position to model scan-dependent corrections. Channels 4 and 5 allow for a different offset and scan-dependent bias over ocean and land/sea-ice. Channels 3 and 4, which are used for cloud detection and the surface emissivity retrieval over land, use just the constant and scan correction terms. Channel 14, the top-most stratospheric channel of AMSU-A, is used as an anchor and therefore assimilated without a bias correction in our experiments. The bias correction coefficients in all experiments are initialised using values from the operational clear-sky system; further investigation of this initialisation choice is given in appendix A.5.

QC check	CLEAR	CLEAR-ALL	ALL
Blacklist or orography	38.35	40.46	40.77
Cloud screened	10.86	11.81	1.6
Broken window channels so cloud screening can't be done	2.07	0	0
Model hydrometeors not available during the final 15 minutes of the assimilation window	0	0.94	1.19
First guess check	0.41	1.6	0.51
Surface check (see section 2.4)	0	0	0.93
Obs error too large	0.34	0	0
VarQC	0	0	0.06
Missing values	0	0.03	0.03
Excess SI	0	0	0.02
Bad emissivity	0	0	0
Negative humidity	0	0	0
Assimilated	85529	80259	97607

Table 4: Summary of the percentage of AMSU-A channel 5 observations which fail various quality control checks in CLEAR, CLEAR-ALL and ALL for one DA window from 21z 31st May 2017 to 09z 1st June 2017. The screening procedures are not progressive, so a single observation can trigger multiple quality control checks. However, for the purposes of the table, the screening is treated as progressive and only the most 'dominant' quality control check is chosen in cases where multiple quality control checks are triggered for a single observation

3 Experiments

Assimilation experiments were conducted to investigate the all-sky assimilation of AMSU-A compared to the clear-sky approach. The experiments were run over two periods of three months each: 1st June 2017 to 31st August 2017 and 1st December 2017 to 28th February 2018. The experiments used the configuration of cycle 45r1 of the IFS and ran at $T_{CO}399$ (28km) forecast resolution with the first, second and third inner loops of the assimilation minimisation run at T_L95 (170km), T_L159 (120km) and T_L255 (80km) resolutions respectively.

The following experiments were conducted: DENY does not assimilate any AMSU-A data and provides a baseline to compare all other configurations to. This should give some context when comparing the various different AMSU-A assimilation methods. CLEAR assimilates AMSU-A in the clear-sky system similar to operations, with modifications discussed below. CLEAR-ALL assimilates AMSU-A through the all-sky system but with a clear-sky methodology including cloud screening and the use of clear-sky radiative transfer modelling. ALL assimilates AMSU-A through the all-sky system with an all-sky methodology including the variable observation error model and all-sky radiative transfer modelling. CHAN4 additionally assimilates AMSU-A channel 4 in the all-sky system on top of the ALL configuration which assimilates channels 5 to 14.

In all experiments slant-path radiative transfer (Bormann, 2016) and constrained VarBC (Han and Bormann, 2016) are turned off for consistency as neither of these features are currently available in the all-sky system. Both of these features are currently part of the operational clear-sky assimilation, and in

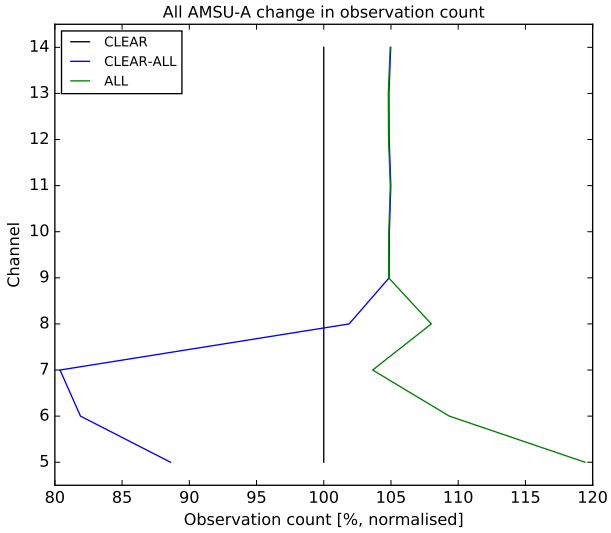

Figure 7: Number of AMSU-A observations assimilated in CLEAR (black), CLEAR-ALL (blue) and ALL (green) experiments for each channel normalised by the number of observations assimilated in the CLEAR experiment. Statistics are accumulated for the period from 21UTC on 9th June 2017 to 21UTC on 19th June 2017.

both cases are reverted to the operational practice before these enhancements were introduced. That is, the slanted viewing geometry is neglected and channel 14 of AMSU-A is assimilated without bias correction. Both enhancements could also be introduced in the all-sky system in the future. As their effects are small for the lower troposphere where all-sky effects are expected to play the largest role, significant interaction is not expected. For all experiments, the AMSU-A bias correction coefficients are initialised from the same spun-up clear-sky values to avoid any spin-up period or large bias differences.

Figure 7 gives an overview of the number of AMSU-A observations assimilated per channel in the three experiments with AMSU-A assimilation. Compared to the CLEAR experiment, there is a 5-20% increase in the number of AMSU-A channels 5-8 observations assimilated in ALL, with the largest increase for the lowest-peaking channel as expected. An increase of around 5% is also present for the stratospheric channels, and this is due to remaining differences in the thinning between the all-sky and the clear-sky system discussed earlier. Figure 8 shows that the number of AMSU-A channel 5 observations assimilated is increased all over the globe but particularly over the storm tracks in the extra-tropical oceans and the Sahara desert. The increase in assimilated observations over the storm tracks is expected due to large areas of frontal cloud where observations are screened out in CLEAR but are assimilated in ALL. The increase over the Sahara desert is because the channel 4 departure check used for cloud screening in CLEAR also acts to quality control for inaccurate surface emissivity or skin temperature used in the radiative transfer calculation. Many observations are rejected due to large departures in channel 4 in the CLEAR system over the Sahara, and without such a check, significantly more observations are assimilated here in ALL. The cloud detection acting to protect the atmospheric analysis from surface-related biases is a similar effect to the one described in section 2.4 over snow and sea ice and is covered in more detail by Bormann et al. (2017). Figure 7 also shows that the number of observations assimilated in the CLEAR-ALL experiment is lower than in CLEAR (by 10-20%), due to the simplified and more cautious cloud detection used in this experiment.

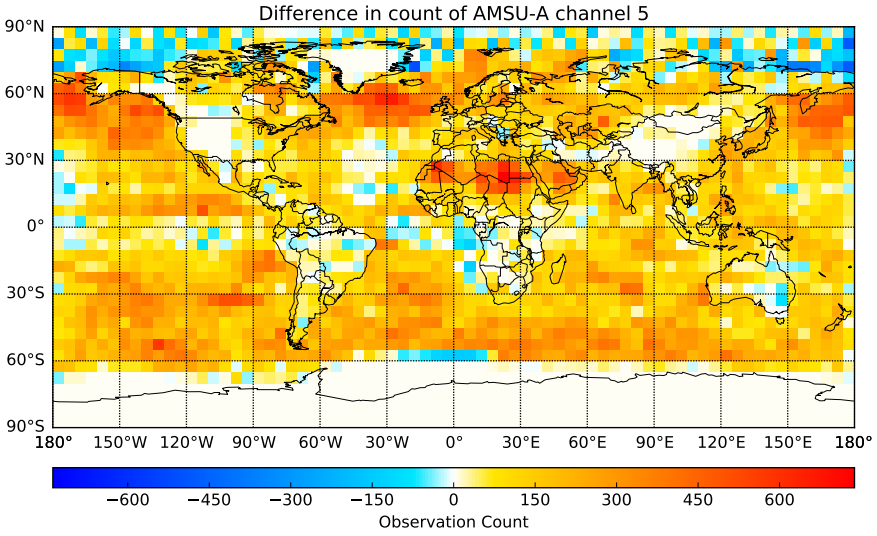

Figure 8: Global distribution of the difference in number of AMSU-A channel 5 observations assimilated between ALL and CLEAR experiments. Statistics are accumulated for the period from 21UTC on 30th June 2017 to 21UTC on 9th July 2017.

4 Results

In this section the results will be presented in three parts. Firstly, the ALL and CLEAR experiments are compared to the DENY experiment to compare the overall impact of AMSU-A when assimilated through the clear- and all-sky systems. Secondly, the differences between CLEAR and ALL will be investigated further by comparing both to the CLEAR-ALL experiment. The aim of these comparisons is to separate the impacts of the remaining differences between the systems from the impacts coming from the assimilation of the additional cloud-affected data. Finally, the CHAN4 and ALL experiments will be compared to assess the impact of the all-sky assimilation of AMSU-A channel 4 which is not currently assimilated in the clear-sky system.

To assess whether forecasts are improved or degraded by the various configurations tested, two main methods of evaluation are used:

1. Change in first guess fits to independent observations: The change in standard deviation of first guess departures to independent observations indicates the change in short-range forecast accuracy. For example, if the standard deviation is increased for sonde temperature then that indicates that the short-range temperature forecasts are degraded as they do not agree as well with the independent sonde measurements after the change

2. Forecast scores against own analyses: Forecast scores for an experiment-control pair are calculated by calculating the RMS error between the forecasts and that experiment's own analyses. The difference between the RMS errors of the experiment and control then indicates whether the experiment has improved or degraded forecasts compared to the control

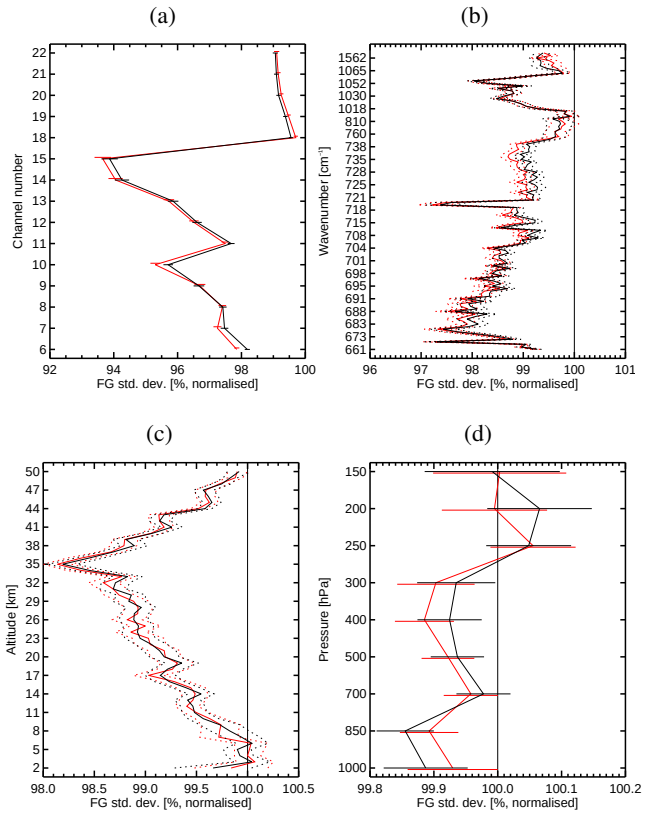

Figure 9: Change in global standard deviation of first guess departures for (a) ATMS, (b) CrIS, (c) GPSRO, (d) atmospheric motion vectors (AMVs), for the CLEAR (red) and ALL (black) experiments against the DENY experiment

4.1 AMSU-A impact in CLEAR and ALL

Comparing CLEAR and ALL to DENY shows the overall impact of AMSU-A in the two systems, respectively, and therefore allows to put the differences between CLEAR and ALL into the context of the overall impact of AMSU-A. Figure 9 shows that the impact of AMSU-A in the clear- and all-sky systems is large and broadly similar on global short-range temperature, humidity and wind forecasts. There are a few differences where CLEAR has a more positive impact than ALL and vice versa, but put into the context of the overall impact of AMSU-A these differences are relatively small. The differences between CLEAR and ALL will be discussed in more detail in the next sub-section, but the results already suggest that the all-sky system is able to replicate most if not all of the impact of AMSU-A on short-range forecasts.

For the extra-tropics, the similar impact seen in the short-range forecasts also translates to similar medium-range forecast benefits (Fig. 10). Both systems show strong statistically significant reductions of the forecast errors from AMSU-A out to day 5-8, depending on hemisphere. The impact is not statistically significantly different in the two systems, as indicated by the overlapping confidence intervals shown. These findings are similar for other geophysical variables and levels in the extra-tropics.

In contrast, the findings for the medium-range forecast impact in the tropics are less clear. Here, Fig. 11 shows that the impact on low-level wind and temperature forecasts in the ALL experiment is significantly smaller than in the CLEAR experiment. However, it is also apparent that the forecast benefit in the

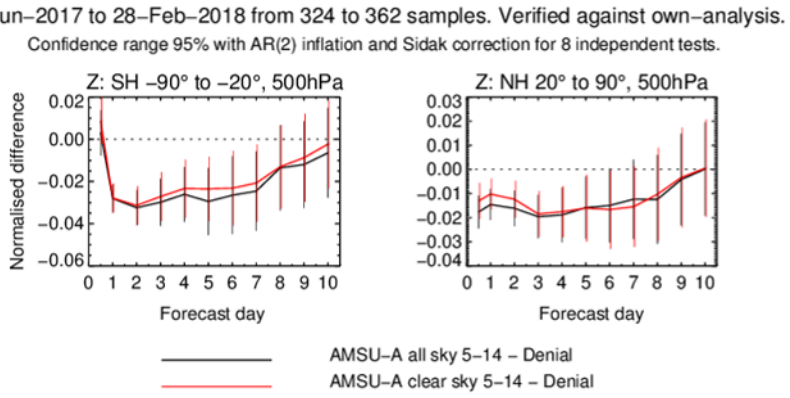

Figure 10: Change in RMSE of 500hPa geopotential height forecasts verified against own analyses for the CLEAR experiment (red) and the ALL experiment (black) against the DENY experiment for the Southern extra-tropics (left) and Northern extra-tropics (right)

CLEAR system is mostly statistically not significant in the tropics at these levels. It is also worth noting that all-sky experiments have been hampered by verification artifacts in the tropics in the past (Geer and Bauer, 2010). These are caused by features being introduced in the analyses that are not carried forward into the forecasts. Then, when the forecasts and analyses are compared the forecasts can look worse. The presence of these artifacts can be confirmed by looking at verification against an independent references (e.g. operational analyses or observations). The reasons behind the apparently poorer impact in the ALL experiment in the tropics will be explored in more detail in the following section 4.2.

Overall, the results highlight that the all-sky assimilation of AMSU-A now largely replicates the performance of the clear-sky assimilation in the extra-tropics, where the forecast impact of AMSU-A is largest. This is an important stepping stone towards achieving additional benefits from the all-sky assimilation. Over the tropics, however, the clear-sky impact of AMSU-A is much smaller, and the all-sky treatment appears to lead to small degradations. These aspects will be investigated in more detail in the next section.

4.2 Comparison of ALL, CLEAR-ALL and CLEAR

In this section the differences between ALL and CLEAR are analysed in more detail, by comparing these two experiments directly. The aim is to characterise better the different performance in the extra-tropics and tropics noted in the previous section, to highlight benefits of the all-sky treatment, and to investigate areas of degradation where further development is needed. To assist with the analysis comparisons to the CLEAR-ALL experiment are also included. This isolates the effects of assimilating additional cloud- and precipitation-affected AMSU-A radiances, and also helps to attribute signals due to different choices and features in the all-sky and clear-sky systems. As highlighted in the previous section, differences in the forecast performance between the two systems are relatively small, especially in the extra-tropics, where few differences are statistically significant. In the following, specific aspects where some consistent signals can be identified are focused on, with some focus on the performance of the short-range forecasts as evaluated through other observations.

The most consistent signal for short-range forecast improvements when comparing the ALL and the

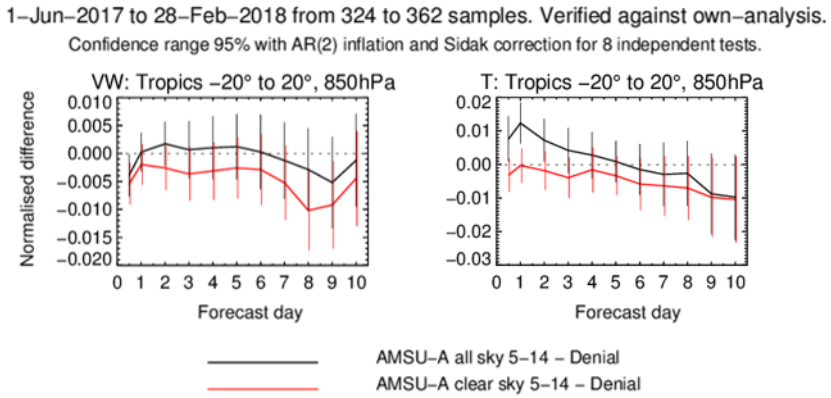

Figure 11: Change in RMSE of 850hPa vector wind (left) and temperature (right) forecasts verified against own analyses for the CLEAR experiment (red) and the ALL experiment (black) against the DENY experiment

CLEAR experiment can be seen for humidity-sounding channels from IR and MW observations assimilated in clear-sky, particularly in the extra tropics. For instance, Fig. 12b shows small, but significant improvements for the humidity sounding channels of CrIS (wavenumbers around 1562cm^{-1}), and Fig. 12c shows similar improvements for the ATMS humidity-sounding channels (18-22) over the Southern Hemisphere. In contrast, the CLEAR-ALL experiment shows a neutral or slightly degraded performance compared to CLEAR here, with the slight degradations possibly a result of fewer tropospheric AMSU-A observations being used. The improvement in the ALL experiment can therefore be attributed to the extra observations being assimilated in this experiment. This could be the result of making better use of the weak low-level humidity information contained in channel 5 of AMSU-A. In addition, the all-sky assimilation of AMSU-A may also help to distinguish between humidity and cloud signals in the assimilation of the humidity-sounding channels in areas of weak cloud signal. Consistent with these interpretations, some MW imager channels assimilated in all-sky do show signs of improvement (e.g., Fig. 12a), suggesting improvements for low-level clouds or possibly total column water vapour. Possibly linked to this are faint improvements for low-level wind forecasts (e.g., Fig. 12d), though this signal is not very consistent between different observing systems and should hence be treated with caution. In contrast, standard deviations of background departures for humidity-sounding channels assimilated in all-sky show no statistically significant change between ALL and CLEAR. These statistics tend to be dominated by signals from cloud-affected regions, so the finding suggests little improvement in the short-range forecasts of mid and high-level clouds from the all-sky assimilation of AMSU-A.

In contrast to the upper tropospheric humidity, the signal for changes in the quality of the short-range forecasts for tropospheric temperature in the extra-tropics is largely neutral between ALL and CLEAR. The majority of temperature-sensitive observations do not indicate a statistically significant change for mid and upper tropospheric temperature in the extra-tropics, and this includes radiosondes, GPSRO, and the hyperspectral IR sounders (e.g., Fig. 12b). ATMS channel 9, sensitive to upper tropospheric temperature even shows a slight improvement (Fig. 12c). The neutral to positive performance for temperature is a positive result, as there is hence no indication that the cloud signals in AMSU-A assimilated in the all-sky system are degrading the high quality of the mid and upper tropospheric temperature analysis. This was a potential problem for the all-sky assimilation of AMSU-A, and it appears that the assimilation approach used in the all-sky system, particularly the observation error model, is mostly successful in

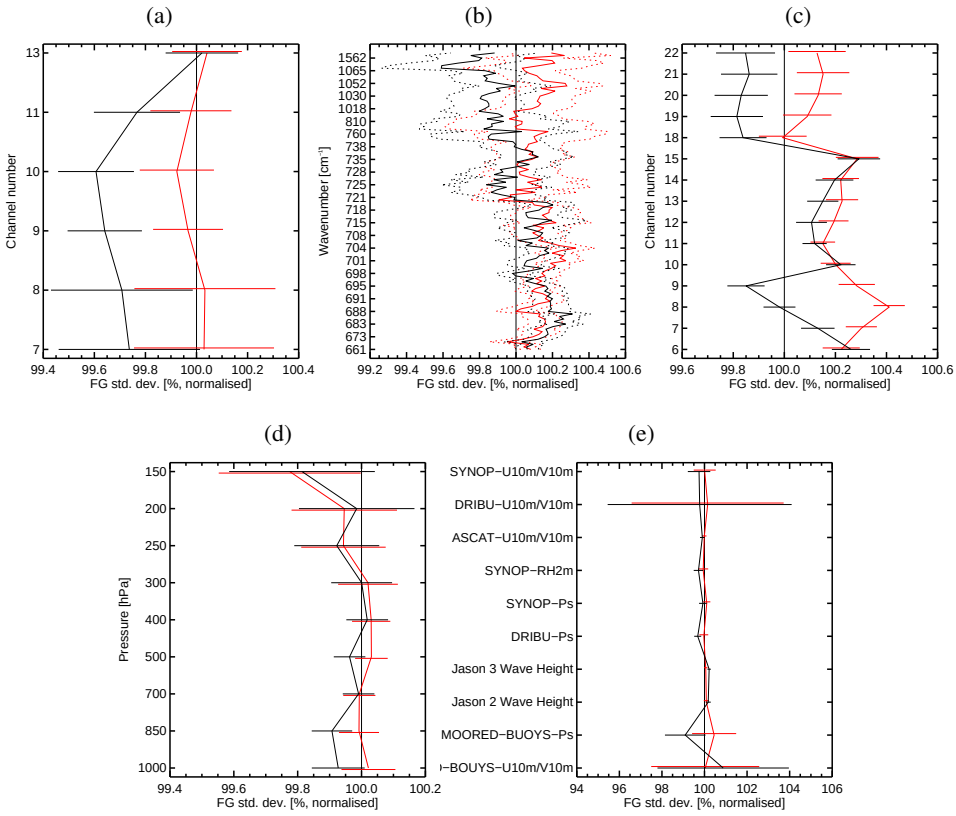

Figure 12: Change in Southern hemisphere standard deviation of first guess departures for (a) AMSR2, (b) CrIS, (c) ATMS, (d) AMVs, (e) conventional surface observations, for the ALL (black) and CLEAR-ALL (red) experiments against the CLEAR (100%) experiment

preventing this, at least for the extra-tropics. Note that the CLEAR-ALL experiment shows a clear degradation compared to CLEAR here, probably a result of the more cautious and simplified cloud detection applied. The finding suggests that the CLEAR experiment, with the more sophisticated cloud detection and observation error model, still manages to extract useful information from using more observations than the CLEAR-ALL experiment.

The situation is different for the lower troposphere in the extra-tropics, where the lowest ATMS temperature-sounding channels exhibit a small degradation in the ALL experiment compared to CLEAR (e.g., Fig. 12c). These appear to be also present in the CLEAR-ALL experiment in which they could be the result of fewer observations being used. However, the finding that the signal is present in both experiments run with the all-sky system may also suggest that it is at least partially due to remaining differences in the clear-sky and all-sky systems unrelated to the use of cloud- and rain-affected observations. For instance, the CLEAR system benefits from the use of the skin temperature sink variable, and this is not used in the all-sky system and would particularly affect the assimilation of these lowest channels.

The evaluation of the short-range forecast performance against ATMS also reveals another aspect, an apparent small degradation in the fit against stratospheric temperature channels in the ALL experiment compared to CLEAR. The signal is also present in IR channels sensitive to the stratosphere (e.g., Fig. 12b), and it is also present in the CLEAR-ALL experiment. This suggests that it is again the result of remaining differences in the clear-sky and all-sky systems unrelated to the use of cloud- and rain-affected observations. One such difference is the different distribution of observations across the scanline (see

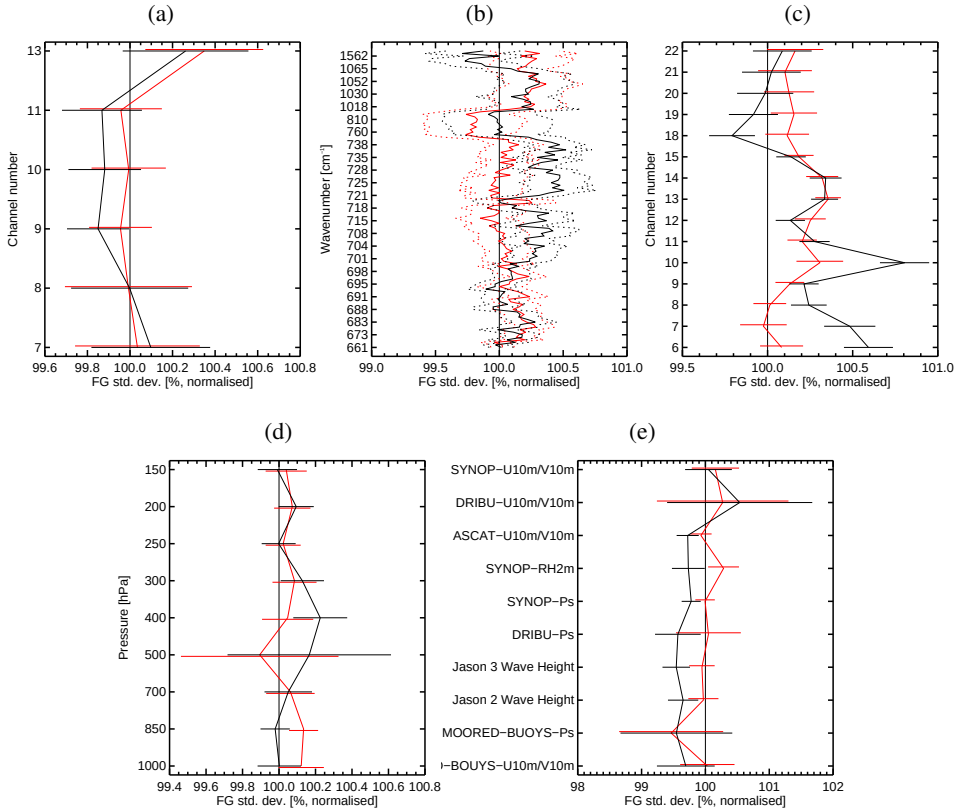

Figure 13: Change in tropical standard deviation of first guess departures for (a) AMSR2, (b) CrIS, (c) ATMS, (d) AMVs, (e) conventional surface observations, for the ALL (black) and CLEAR-ALL (red) experiments against the CLEAR (100%) experiment

Fig. 4) which possibly contributes to the degradations seen here, as the all-sky system will have smaller spacing between the observations of the scan-positions close to nadir, thus being more prone to being affected by neglected spatially correlated observation errors. Figure 27 in appendix A.3 highlights the sensitivity of the short-range forecast quality when measured against ATMS to changes in the AMSU-A all-sky thinning configuration. This provides evidence that any remaining differences between the clear- and all-sky thinning could lead to impacts of the same magnitude as seen in Fig. 12c. This could also provide an alternative explanation of the poorer CLEAR-ALL performance seen in the tropospheric temperature-sounding channels in ATMS, and hence may offer scope for further optimisation of the all-sky system. Note, however, that the slightly poorer performance seen in the stratosphere does not seem to translate to a poorer medium-range forecast performance (not shown), and it is thus of a lesser concern.

For the tropics, the short-range forecast performance of the ALL experiment is overall less favourable with one notable exception. Figure 13e shows improved fits to a number of conventional surface observations including surface pressure, humidity, wind and wave observations. In particular, the improvements to surface pressure are a good indication of improvements to the synoptic state of the atmosphere. However, despite this indication, the impact on cloud and upper tropospheric humidity is much more neutral than in the extra-tropics as suggested by the fits to the MW imaging channels of AMSR2 (Fig. 13a), and the humidity sounding channels of CrIS (Fig. 13b) and ATMS (Fig. 13c). In addition, the low-level wind fits are also more neutral in the tropics (Fig. 13d). The fits to other temperature-sensitive MW and IR observations are generally degraded in the tropics. For instance, Figs. 13b and c show considerable degra-

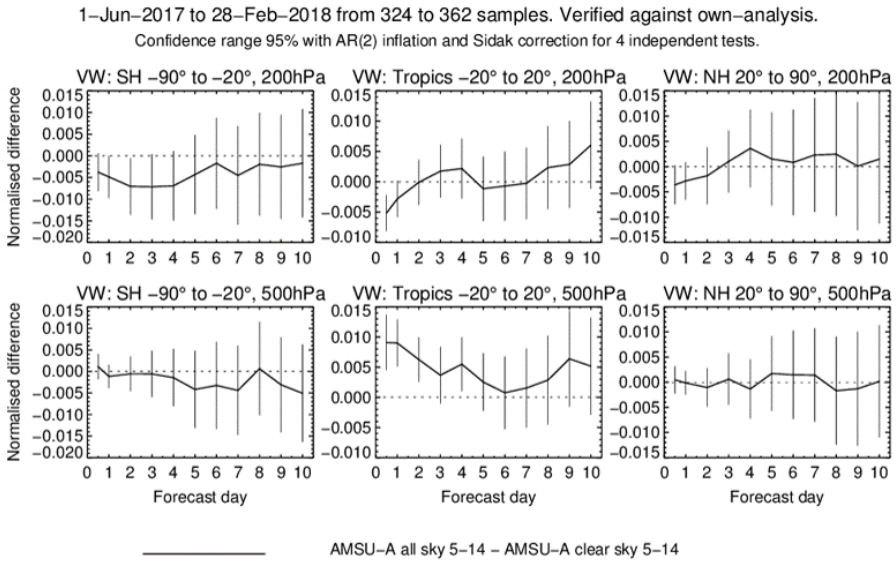

Figure 14: Change in vector wind forecast RMSE from T+12 to T+240 in the Southern hemisphere extra-tropics (left), tropics (middle) and Northern hemisphere extra-tropics (right) at 200hPa (upper) and 500hPa (lower) when comparing ALL to CLEAR

dations in the standard deviation of background departures for the tropospheric temperature-sounding channels of CrIS and ATMS in the ALL experiment compared to CLEAR. These are not present in the CLEAR-ALL experiment, and can hence be attributed to the use of the additional observations in the all-sky system. While these degradations are relatively small, and other observations show no degradations, they nevertheless indicate a slightly poorer performance of the all-sky system in the tropics. As discussed further below, the more aggressive use of observations over the Sahara noted earlier (e.g., Fig. 8) appears to be at least partially responsible for this. Another aspect could be larger representation errors for convective clouds prevalent in the tropics, as discussed in section 2.2, and this aspect is not currently included in the observation error model used.

The pattern of slight improvements in the extra-tropics and degradations in the tropics appears to be consistent into the medium-range. Figure 14 shows that for vector wind there are areas of improvement on the borderline of statistical significance in the extra-tropics, particularly at 200hPa in the Southern hemisphere. These improvements may be linked to the improvements in humidity noted in the short-range forecasts. In the tropics there are significant degradations at 500hPa, particularly at the shorter forecast ranges and these appear to be backed up by degraded fits of short-range forecasts to AMVs (Fig. 13d).

The slightly improved forecasts in the Southern hemisphere are mostly located in the storm tracks (not shown). This is an area where there is a significant increase in the number of AMSU-A observations assimilated as shown in Fig. 8. One explanation for these improvements is due to the 4D-Var tracing effect where misplaced cloud and precipitation features have their position corrected by adjustments to the wind-field earlier in the assimilation window. This is the main mechanism behind the positive impact of the existing all-sky assimilation of the microwave imaging and humidity sounding channels.

The slightly poorer performance in the tropics can, to some extent, be traced back to issues with the treatment of surface-sensitive channels over land in the all-sky system. For instance, Fig. 15 shows

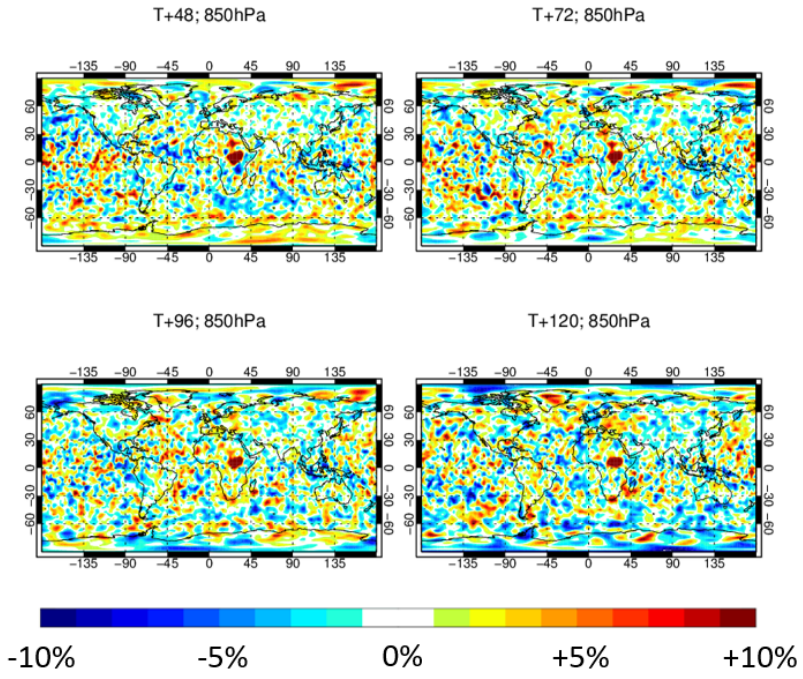

Figure 15: Map plots of the change in 850hPa temperature forecast RMSE at T+48, 72, 96 and 120 hours when comparing ALL to CLEAR. Note that no statistical significance testing is applied for technical reasons

considerable areas of apparent degradation over Africa at all forecast ranges for 850hPa temperature forecasts. The signal is also present in the CLEAR-ALL experiment (not shown), albeit to a lesser extent, and it is linked to considerable changes in the mean analysis over this region (Fig. 16). The changes in the mean analysis are most likely the result of differences in the treatment of surface-sensitive channels between the all-sky and clear-sky system. There are significant diurnal biases in the surface sensitive channels such as AMSU-A channel 5 over arid regions, related to strong diurnal biases in the model skin temperature used (Bormann et al., 2017). In the CLEAR system, the effect of these biases is reduced through removing many bias-affected observations through the window channel departure check and by allowing the skin temperature sink variable to account for some biases. The CLEAR-ALL experiment still uses similar quality control, but does not have the skin temperature sink variable, whereas ALL neither has quality control to protect from these biases, nor a sink variable. Figure 8 indeed shows that there are many more AMSU-A channel 5 observations assimilated over Africa in ALL compared to CLEAR which are likely to be contributing to the degradations seen. This could be addressed by introducing a skin temperature sink variable and developing quality control that rejects observations when the diurnal biases are too strong.

Some of the degradations to vector wind and temperature forecasts also extend over ocean so the lack of a skin temperature sink variable is not solely responsible for the degradations across the tropics. Indeed, the change in ATMS first guess fits are consistently degraded over land and ocean, and there are similar degradations to lower peaking CrIS channels in the tropics (Fig. 13c) which are only assimilated over ocean. This could be caused by the larger representation errors of convective clouds in the tropics (see Fig. 21) which are not taken account of in the current observation error model and could mean that

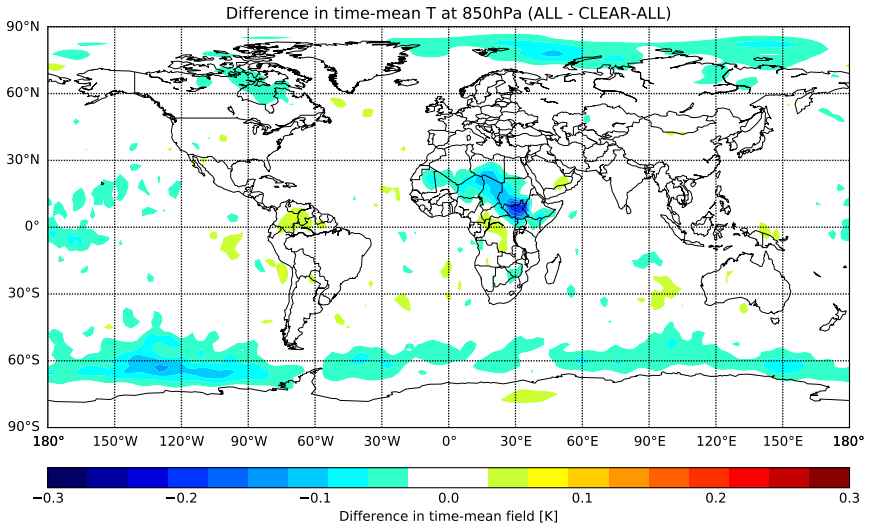

Figure 16: Map showing the mean change to the 850hPa temperature analysis in ALL against CLEAR-ALL

the cloudy AMSU-A observations are being over-weighted here. A possible solution to this would be to account for the different cloudy observation errors with an additional predictor such as total column water vapour, where a larger cloudy observation error would be used in areas of higher total column water vapour.

4.3 Addition of channel 4

In this section the impact of adding AMSU-A channel 4 in the all-sky system will be evaluated. This channel is not currently assimilated in the clear-sky system, as it is relatively strongly sensitive to cloud liquid water, in addition to lower tropospheric temperature and humidity. This makes it a good candidate for all-sky assimilation so the additional assimilation of this channel on top of the ALL configuration is investigated.

An evaluation of short-range forecast impact against other observations suggests mixed results from adding channel 4. Figure 17 shows that there are improved background fits to AMSR2 and low-peaking CrIS channels (wavenumbers between 700 and 1000cm^{-1}). These may indicate improvements in low-level humidity over sea, or better low-level temperature and cloud forecasts. However, there are also degraded fits to AMVs in the lower and upper troposphere and the geostationary IR clear sky radiances. These suggest degraded wind and upper tropospheric humidity forecasts, respectively. These impacts (both positive and negative) are stronger in the tropics and weaker in the extra-tropics.

Figure 18 shows that the temperature forecast scores are improved very close to the surface in the tropics but are significantly degraded in the lower troposphere in the Southern hemisphere, which is also the case for relative humidity (not shown).

Further investigation suggests that the assimilation of channel 4 is likely to be hampered by considerable residual biases for this channel, arising from a too restrictive bias correction model. Figure 19 shows the globally averaged biases for AMSU-A channel 4 which appear to map onto air mass biases. The bias model used for AMSU-A channel 4 does not include air mass bias predictors, so these cannot be

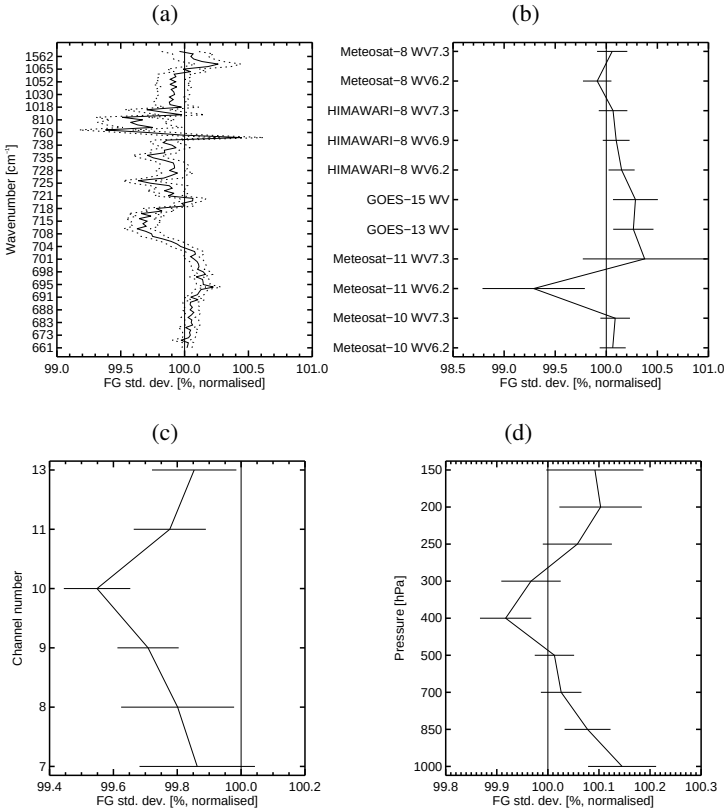

Figure 17: Change in global standard deviation of first guess departures for (a) CrIS, (b) Geostationary IR clear sky radiances, (c) AMSR2, (d) AMVs, for the CHAN4 experiment against the ALL experiment

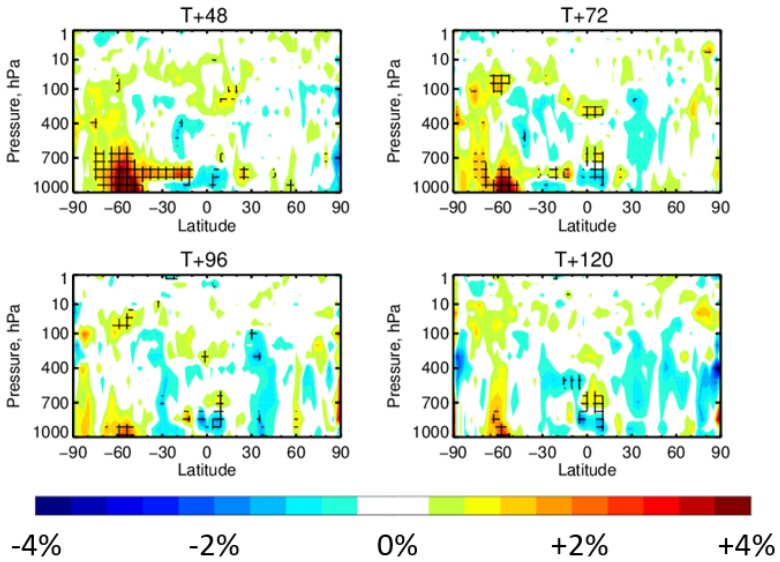

Figure 18: Latitude-pressure plots of the change in temperature forecast RMSE at T+48, 72, 96 and 120 hours when comparing CHAN4 to ALL

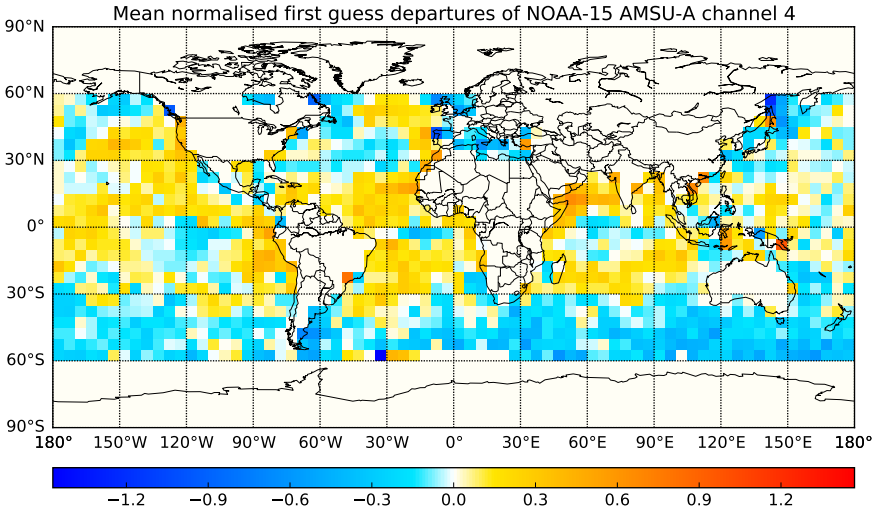

Figure 19: Maps of NOAA-15 AMSU-A channel 4 mean first guess departures after bias correction divided by observation error. Statistics are accumulated for the period from 21UTC on 30th June 2017 to 21UTC on 9th July 2017.

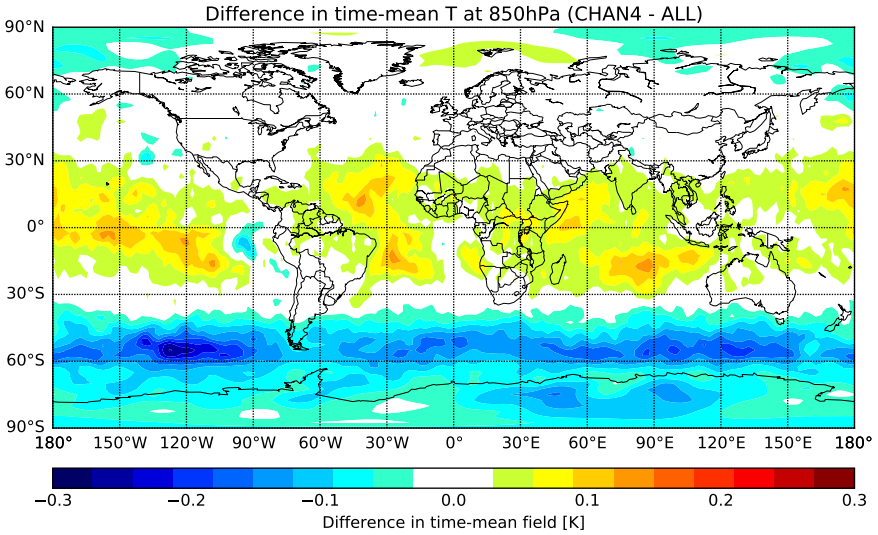

Figure 20: Map showing the mean change to the 850hPa temperature analysis in CHAN4 against ALL

corrected by VarBC. Figure 20 shows that assimilating AMSU-A channel 4 results in a mean warming to the analysis and forecasts at 850hPa over the tropical oceans and a mean cooling over the Southern extra-tropics. This pattern of warming and cooling appears to correlate very strongly with the residual biases and suggests that the residual biases are dominating the changes that channel 4 is able to make to the analysis.

Previous work to assimilate AMSU-A channel 4 was also hampered by the effects of residual biases (Geer et al., 2012) so perhaps these problems could be addressed by revisiting the bias predictor model used for AMSU-A channel 4. In particular the use of some air mass bias predictors, such as the ones

used for the higher peaking sounding channels, could be investigated.

5 Conclusions and future work

The all-sky assimilation of AMSU-A has been investigated. The results when comparing both clear- and all-sky configurations against the denial suggest that in the context of the overall impact of AMSU-A the performance of the two assimilation approaches is rather similar. In particular, the all-sky system replicates and in some cases improves the clear-sky impact in the extra-tropics, where the impact of AMSU-A is largest. In these regions, the results suggest, for instance, improvements in the short-range forecasts of tropospheric humidity, low-level winds and clouds. These improvements are small but they are statistically significant when assessed via first guess fits to independent observations. There are also small improvements into the medium-range in the extra-tropics although they are not statistically significant. Even so, this is an encouraging result and one potential explanation for it is the 4D-Var tracing effect.

The all-sky benefit in the tropics is less clear. There are indications of slight degradations for tropospheric temperature and wind. The former is especially the case over Africa, and this is possibly related to the absence of the skin temperature sink variable in the all-sky system. One other possible explanation is that the cloudy observation errors are global averages and there is evidence, see Fig. 21, that these errors are larger in the tropics and smaller in the extra-tropics. NWP models are better at predicting frontal cloud and precipitation than convective cloud and precipitation (Ebert et al., 2007). The all-sky observation error model is designed to account for observation, model and representation errors so it follows that the cloudy observation errors will be larger in areas where there are larger model and representation errors such as in convection. Hence, in the current all-sky observation error model, it's possible that the observations are over-weighted in the tropics which could explain the degradations seen.

Despite the minor degradations in the tropics, the results are overall very encouraging and suggest that the operational all-sky assimilation of AMSU-A is feasible. The results could be used to motivate a strategy that future microwave sounding instruments, such as MWS on EPS-SG, should be assimilated through the all-sky system. These combine temperature and humidity-sounding channels, and a dual implementation in the clear-sky and all-sky systems is undesirable. At the same time, the remaining small degradations in forecast performance in the tropics against the denial are still important to understand and improve to maximise the impact from AMSU-A and any future instruments. Also, given clear benefits from moving to an all-sky assimilation of AMSU-A in other systems (e.g., Migliorini and Candy (2019)), clearer benefits might have been expected. However, the clearer benefits at other centres were achieved in the context of no other MW radiances assimilated in an all-sky approach, whereas clouds are already much better constrained in the present ECMWF analysis through the extensive use of humidity-sounding radiances in all-sky. Adding further constraints on clouds will therefore necessarily show smaller benefits in the ECMWF system.

The additional assimilation of AMSU-A channel 4 in the all-sky systems currently gives mixed results, with improved short-range near-surface forecasts but degraded forecasts in the upper atmosphere. It appears that residual biases are playing a role here which would need to be addressed to obtain improved results. Nevertheless, this is an example where all-sky assimilation of AMSU-A offers further opportunities and these should be pursued further in the future.

The work documented in this report built on the work of Geer et al. (2012) and successfully addressed some of the issues identified. For instance the clear- and all-sky systems have been made much more consistent in terms of the quality control, thinning and bias correction configurations. This reduces the

impact of these primarily technical differences between the two systems and allows the clear-sky and all-sky assimilation of AMSU-A channels 5-14 to be broadly similar in performance. However, there are still improvements required to switch to all-sky assimilation operationally and some of the same issues remain, such as the mean changes to the analysis dominating the impact when assimilating AMSU-A channel 4.

Many of the issues covered in appendix A and the resulting impacts of changing and correcting the configuration highlight the sensitivity of the AMSU-A assimilation configuration. AMSU-A consistently ranks as the instrument which yields the most impact on forecast accuracy both in FSOI and OSEs and the results when comparing to the denial experiment show the large positive impact from assimilating the data. Therefore, even relatively minor technical choices in the configuration can make a significant difference to the forecast performance. A large part of this work was spent optimising aspects of the all-sky configuration that appear to make little difference for the all-sky assimilation of the microwave imagers and humidity sounders. Two enhancements motivated by the AMSU-A configuration which have now been applied more widely across the all-sky system are the assimilation over coasts (Weston et al., 2017) and the interpolation method (appendix A.2). These both gave small but significant improvements and there is potential that some of the other unique aspects of the AMSU-A all-sky configuration could be applied to the all-sky system as a whole to yield further benefits. The present work also highlights the sensitivity of the AMSU-A assimilation to thinning choices, particularly in the context of having observations from seven different satellites. Two aspects which made a considerable difference to the numbers and distribution of AMSU-A observations assimilated were the threshold on how far the observations were from the T_L255 reduced Gaussian grid points and whether the different satellites were thinned together or separately. Changing these aspects both had significant effects on the forecast quality, see appendix A.3 for details.

The present work has also identified several areas that should be investigated further, and are likely to improve the remaining small degradations seen in the all-sky assimilation of AMSU-A:

1. Thinning: As mentioned in section 2.3 and appendix A.3 many of the differences between the thinning in the clear- and all-sky systems have been addressed. However, there are remaining differences which result in a different sample of observations across the scan, in particular fewer observations near the edge of the scan are used in ALL compared to CLEAR (Fig. 4). When MHS was moved from the clear-sky system to the all-sky system it was found that the activation of observations near the edge of the scan resulted in a significant increase in the overall impact of MHS (Geer et al., 2014). Therefore, addressing this difference has the potential to increase the impact of AMSU-A in the all-sky system. This could be done by using observations closest to every point of a T_L159 reduced Gaussian grid as opposed to the current method which uses observations closest to alternative points of a T_L255 reduced Gaussian grid. The maximum distance threshold of 30km could also be relaxed when using the lower resolution grid. The proposed method would result in an average separation distance of 123km which is very close to the current clear-sky thinning separation distance of 125km and should result in a much more similar sample of observations across the scan between the clear- and all-sky systems.

2. Refinement of the observation error model: When constructing the observation error model, it was found that when sampling data from different latitude bands the resulting histograms of standard deviation of first guess departures against cloud amount looked quite different. Figure 21 shows that when considering only data in the high latitudes the value at which the cloudy error saturates is much lower than the same value when only considering observations in the tropics. This is related to the different cloud regimes present in these two meteorologically diverse areas and

different representation errors associated with them. In the tropics there will be many convective clouds leading to enhanced scattering by ice particles and hence large variability in the first guess departures when cloud is present. In high latitudes frontal cloud dominates where there is less scattering leading to smaller variability in the first guess departures in cloudy areas. Currently a globally averaged observation error model is used but taking account of this additional variability may yield better results, particularly in the tropics where it is possible the observations are being over-weighted in areas where convective clouds are present. In the new microwave imager correlated observation error model, total column water vapour is used as an additional predictor to help account for this effect (Alan Geer, personal communication), so something similar could be implemented for AMSU-A.

3. Skin temperature sink variable: This is currently present in the clear-sky system but not in the all-sky system. There is ongoing work to replace this methodology as ECMWF moves to a more coupled assimilation strategy between the atmosphere, land surface and ocean. However, results from experiments to remove the skin temperature sink variable in clear-sky (Cristina Lupu, personal communication) show similar signatures in forecast scores over Africa that have been seen in section 4 here. Therefore, enabling the skin temperature sink variable could yield better near-surface temperature forecast results in the tropics where some of the biases in the surface sensitive channels would influence the skin temperature instead of the lower atmospheric analysis and short-range forecasts. One concern with using the skin temperature sink variable in all-sky is that there is a danger that real cloud signals in the departures could be aliased into skin temperature increments, thus losing the potential benefit of this sensitivity in the atmospheric analysis. In this context, recent developments at ECMWF to use skin temperature background errors that better reflect the situation-dependent uncertainty in the skin temperature background are likely to help with the attribution of such signals. Refined quality control where diurnal biases in the lowest sounding channels are particularly large (e.g., in arid regions) may also be required.

4. Channel 4 departure as over land predictor: The 23-89GHz scattering index which is used as the cloud predictor for the error model over land is primarily sensitive to frozen hydrometeors because of the enhanced scattering at 89GHz over 23GHz. It is relatively insensitive to cloud liquid water and rain whereas channel 5 is primarily sensitive to liquid cloud and precipitation. This could potentially lead to the situation where, in areas of exclusively liquid cloud over land, channel 5 is over-weighted as the scattering index is insensitive to liquid hydrometeors. One alternative is to use the channel 4 departure as the cloud predictor over land. This is currently used as the primary method of cloud detection in the clear-sky system over land and is sensitive to cloud and precipitation in the liquid phase. Figure 22 shows that the standard deviation of first guess departures for channel 5 do vary linearly with channel 4 departure so using this as the cloud predictor over land could be a possible enhancement over the current method. This would also offer some protection against the surface-related biases seen in section 2.4.

There are also other refinements that could be investigated and may offer benefits for the general all-sky assimilation of AMSU-A. These aspects may also help to address present short-comings, and they are primarily motivated by experience gained with the assimilation of humidity-sounding instruments in all-sky:

1. Variational quality control (VarQC, Anderson and Järvinen (1999)): It has been found that VarQC plays an important role in the assimilation of the MW imagers and humidity sounders in all-sky (Geer and Bauer, 2011). VarQC is turned on for AMSU-A in both clear-sky and all-sky but it

(a)

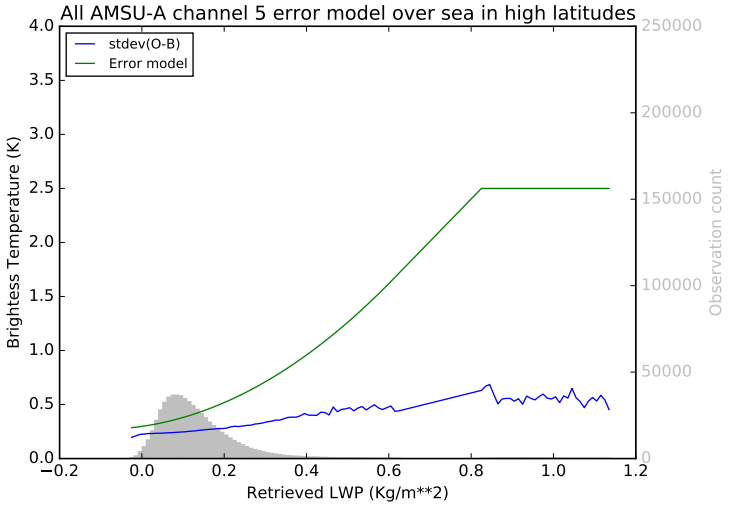

(b)

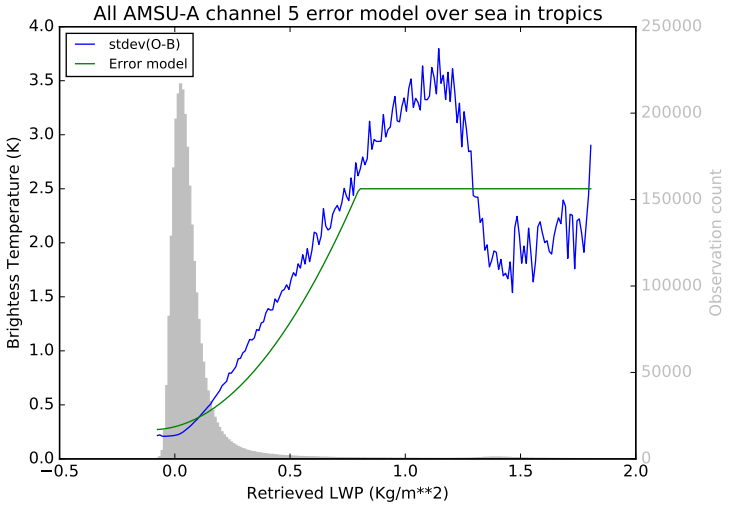

Figure 21: Standard deviation of AMSU-A channel 5 first guess departures binned against retrieved cloud liquid water over ocean considering only observations from: (a) high latitudes with latitude $>60°$; (b) tropics with latitude $<30°$

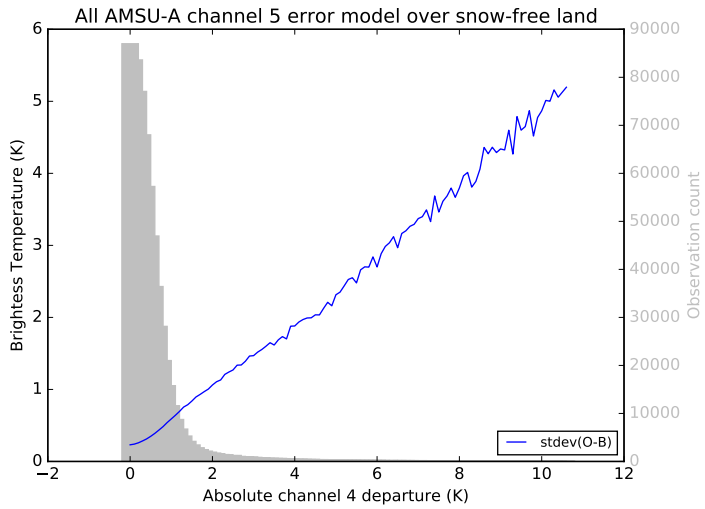

Figure 22: Variability of the standard deviation of AMSU-A channel 5 first guess departures with absolute AMSU-A channel 4 first guess departures as a cloud predictor over land

uses the same loose configuration which means that very few AMSU-A observations are down-weighted or rejected by VarQC in either the clear- or all-sky systems. This may be an optimal configuration in clear-sky but there is the potential for a tighter configuration to yield benefits in all-sky as has been seen in the other all-sky microwave data.

2. Inter-channel error correlations: Previous work has shown that inter-channel error correlations are generally stronger in cloud-affected radiances than in radiances in only clear scenes (Bormann et al., 2011). This would appear to also be the case for AMSU-A as Fig. 23 shows stronger correlations, particularly between channels 5, 6 and 7 in cloudier scenes. Recent work has shown that benefits can be gained by taking account of variable correlated errors in the context of the all-sky assimilation of infrared humidity sounding radiances (Geer, 2019) and microwave imager radiances (Alan Geer, personal communication). Therefore, taking into account inter-channel error correlations for all-sky AMSU-A assimilation could yield similar benefits.

Finally, the present experimentation with AMSU-A in all-sky excluded some refinements to the clear-sky assimilation of AMSU-A, namely the use of slant path radiative transfer and constrained VarBC for channel 14. Both of these are particularly relevant for the assimilation of the stratospheric AMSU-A channels, and the interaction with the all-sky assimilation is expected to be small. Nevertheless, these aspects will need to be addressed before an operational assimilation of AMSU-A in all-sky, by adopting similar methodology in the all-sky system.

Acknowledgements

Peter Weston is funded by the EUMETSAT Research Fellowship programme. Many thanks to Katrin Befort, Heather Lawrence, Cristina Lupu, Stefano Migliorini, Tom Auligné, Kristen Bathmann and Andrew Collard for useful suggestions and discussions. Stephen English is thanked for reviewing the report.

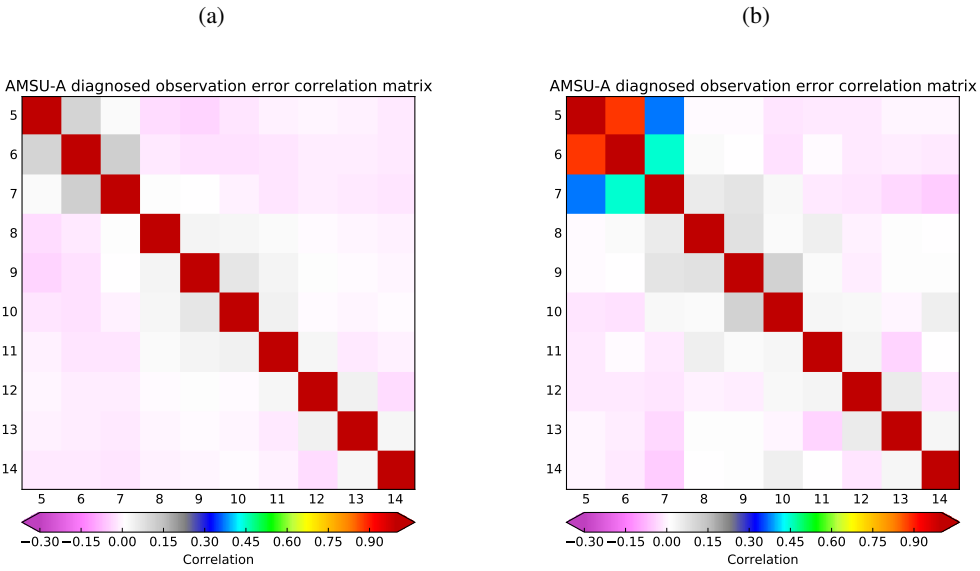

Figure 23: Diagnosed inter-channel error correlations using the method of Desroziers et al. (2005) for AMSU-A (a) only considering scenes with retrieved cloud liquid water between 0.1 and 0.2 kg m^{-2} (b) only considering scenes with retrieved cloud liquid water between 0.8 and 0.9 kg m^{-2}

Appendices

A Removing differences between clear- and all-sky systems

A.1 Quality control differences

Initial comparisons of the number of AMSU-A observations assimilated in the CLEAR and CLEAR-ALL configurations showed significantly fewer observations were assimilated in CLEAR-ALL. This was due to a different set of quality control procedures applied in the all-sky system.

In the all-sky system, all observations were rejected in areas of mixed land and ocean (e.g. surrounding coasts, inland lakes etc.). This was relaxed for the all-sky humidity sounders which resulted in a 10-20% increase (dependent on model resolution) in the number of all-sky observations assimilated (Weston et al., 2017). This was also relaxed for AMSU-A (albeit retaining some coastal blacklisting for channels 5 and 6 also present in the clear-sky system) and the effect on observation numbers was similar.

In the all-sky system, all observations were rejected when the dynamic emissivity retrieval failed and no emissivity atlas value could be used. For non-surface sensitive channels this was relaxed and a dummy emissivity value of 0.55 over ocean, 0.8 over sea ice or 0.95 over land was used. This is now consistent with the clear-sky system and resulted in a 1-2% increase in observations assimilated.

Finally, in the all-sky system some deprecated sea ice screening remained which had already been removed from the clear-sky system. This was also removed in the all-sky system resulting in a $\sim$10% increase in the number of observations from AMSU-A channels 5 and 6 assimilated. A dynamic emissivity retrieval is used over sea ice to provide an accurate surface emissivity estimate to the radiative transfer model. In addition, a constant observation error is used because scattering indices and cloud

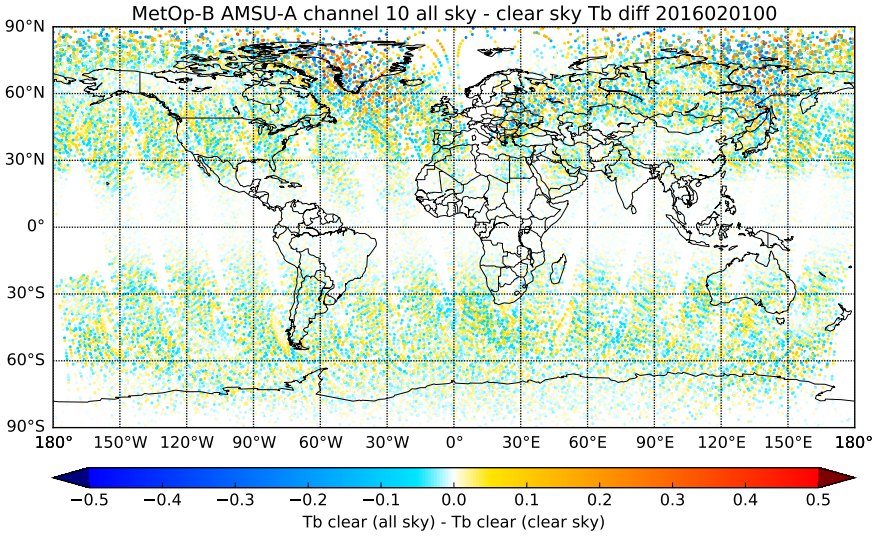

Figure 24: Difference between model equivalents in observation space for MetOp-B AMSU-A channel 10 data between 21UTC on 31st January 2016 and 09UTC on 1st February 2016 from the all-sky and clear-sky systems before the bi-linear intrerpolation was adopted in the all-sky system

liquid water retrievals are inaccurate over sea ice.

Other than changes due to thinning differences, see section A.3, this meant that the number of observations assimilated in the two systems were fairly similar. In particular, the number of observations being rejected by quality control were very similar.

A.2 Interpolation

When the model equivalents in observation space are calculated for all observations a horizontal interpolation is done between the model grid point locations and the observation locations. In the IFS there are several possible interpolation methods and different methods are used depending on the observation types and model variable. In the clear-sky system either a bi-linear or bi-cubic interpolation is used (from model cycle 46r1 the bi-linear interpolation will be used exclusively and the bi-cubic interpolation will be retired). However, in the all-sky system the interpolation was originally done by simply taking the nearest neighbouring model grid point as the value at the observation location.

Using the nearest neighbour method is also a legacy of the early all-sky experiments using the 1D+4D-Var method (Geer et al., 2007) and makes good sense for the cloud hydrometeors as it helps to maintain a physically consistent profile for input into the radiative transfer model. However, for smoothly varying fields such as temperature, the nearest neighbour method could be introducing unnecessary interpolation errors into the first guess departures. The effect of this discrepancy between the systems can be seen when looking at maps of collocated differences between model equivalents at observation locations from the all-sky and clear-sky systems, see Fig. 24. When using a consistent interpolation for all variables (except the cloud hydrometeors and the land-sea mask) in both systems the equivalent maps show that the colocated differences are zero everywhere (not shown).

This also has an effect on the global AMSU-A first guess departure statistics. Figure 25a shows that using the bi-linear/bi-cubic interpolation instead of the nearest neighbour results in a significant reduction in

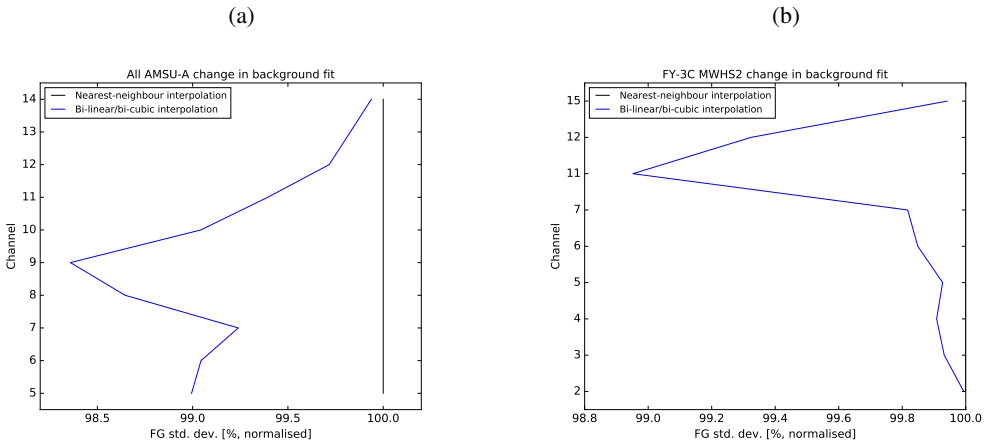

Figure 25: Global change in standard deviation of all-sky (a) AMSU-A and (b) MWHS2 first guess departures resulting from change in interpolation from nearest-neighbour to bi-linear/bi-cubic. The same first guess is used in both cases to isolate the impact of the interpolation change

the standard deviation of first guess departures for all AMSU-A channels, particularly the tropospheric and lower stratospheric channels. This change was also applied to the other all-sky instruments where it had a similar effect on the MWHS2 118GHz temperature sounding channels 2-7 and 183GHz humidity sounding channels 11-15 (Fig. 25b) and also improved fits to other humidity sounding and imaging channels (not shown). The impact on forecast scores of this change was neutral but it meant a much closer match between the AMSU-A first guess departure statistics in the clear-sky and all-sky systems which means it will become the new default from cycle 47r1.

A.3 Thinning

As introduced in section 2.3 there were some significant differences in the thinning procedures between the clear- and all-sky systems in the initial experimentation. One such difference was that in the clear-sky system different satellites are thinned together and in the all-sky system different satellites are thinned separately. Figure 26 shows that the effect of changing from thinning different satellites separately to together on the number of AMSU-A observations assimilated is largest in the high latitudes where the orbit tracks of different satellites overlap. Overall, the distribution of AMSU-A observations in the all-sky system is much more similar to the clear-sky system when the different satellites are thinned together. This also has a significant effect on the accuracy of temperature and humidity short-range forecasts, with significantly improved fits to all ATMS channels, as shown in Fig. 27. The implication is that the forecast accuracy is very sensitive to thinning choices for AMSU-A due to the significant impact that the AMSU-A observations have, as seen in the denial results in section 4.1.

A.4 Bias correction in the emissivity retrieval

When all-sky assimilation was introduced over land at ECMWF the SSMIS radiances used in the dynamic emissivity retrieval were bias corrected to address instrument issues and broad global biases (Baordo and Geer, 2016). AMSU-A does not suffer the same instrument issues as SSMIS so this motivated experiments to test the difference between using bias corrected and non-bias corrected AMSU-A

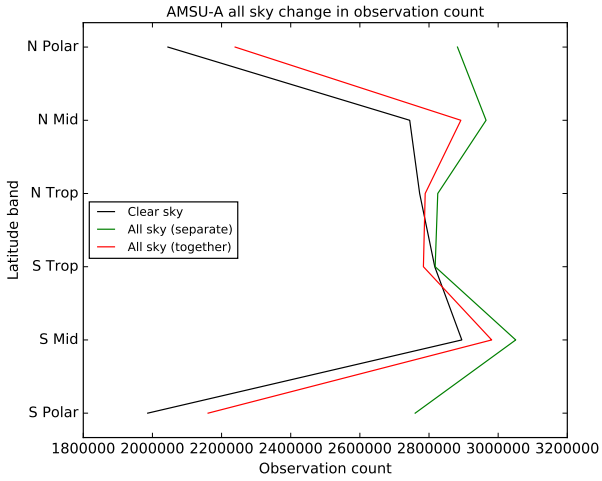

Figure 26: Number of AMSU-A channel 5 observations assimilated (after cloud screening) by latitude band for the clear-sky (black) and all-sky systems when different satellites are thinned separately (green) and together (red). Statistics are calculated for the period from 21UTC on 1st June 2017 until 21UTC on 8th June 2017.

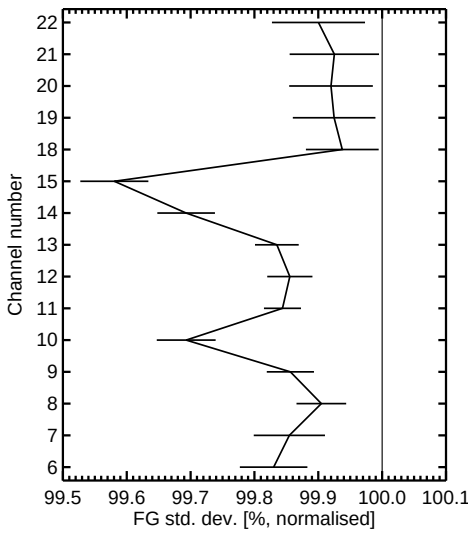

Figure 27: Global change in standard deviation of first guess departures to ATMS when different AMSU-A satellites are thinned together instead of separately in the all-sky system. Experiments were run for a total of 6 months.

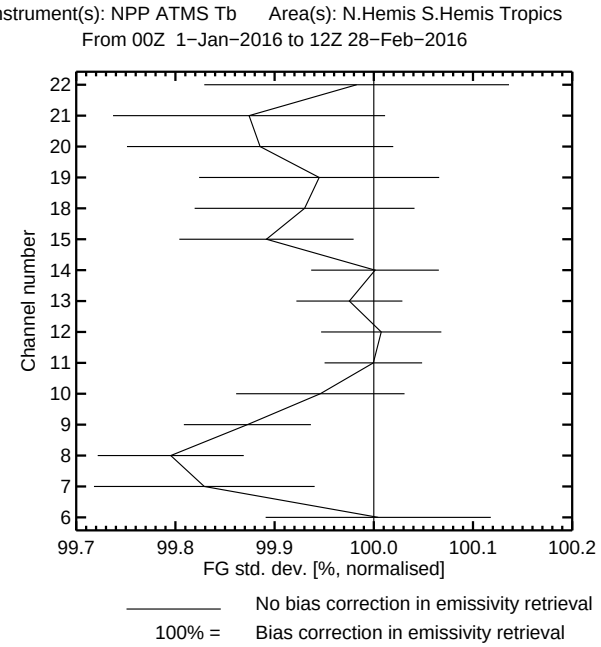

Figure 28: Change in global standard deviation of first guess departures for ATMS when not bias correcting the radiances used in the emissivity retrieval for AMSU-A all-sky assimilation over land

radiances in the emissivity retrieval, as mentioned in 2.4. Figure 28 shows that the first guess fits to the upper tropospheric temperature sounding channels (7-9) are improved, which indicates improved short-range upper tropospheric temperature forecasts when not using a bias correction. Therefore, in all subsequent experimentation the radiances used for the emissivity retrieval were not bias corrected for AMSU-A. The choice could also be revisited for other instruments for which instrument-specific biases are smaller than originally encountered for SSMIS.

This result highlights the difficulty in obtaining high-quality bias corrections for surface sensitive channels which do not have a good estimate of the surface emissivity. An alternative to potentially obtain better quality bias corrections for these channels, would be to simultaneously retrieve the surface emissivity along with the skin temperature.

A.5 Bias correction issues

A.5.1 Window channel predictors

In the first set of AMSU-A all-sky experiments the bias predictors for channels 3 and 4 were inadvertently set to include model skin temperature and total column water vapour. These predictors are used for radiances from microwave imager instruments such as SSMIS, AMSR2 and GMI and are suitable predictors when only considering observations over ocean. However, over land, there are known to be large diurnal model skin temperature biases (Trigo et al., 2015). In the presence of significant model biases, it has been shown that using current variational bias correction schemes can lead to model biases affecting the analysis and subsequent short-range forecasts (Eyre, 2016). This effect led to a positive feedback in the applied bias correction for channel 3 which meant that after two months the applied bias correction had increased to around 7K, see Fig. 29, reflecting the size of model skin temperature biases. This affected the emissivity retrieval (this experiment still used bias corrected radiances in the emissivity

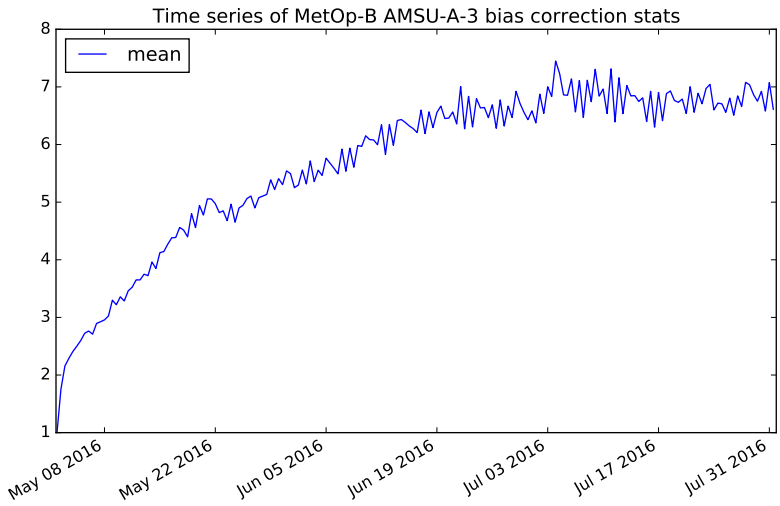

Figure 29: Time series of the applied bias correction (K) for MetOp-B AMSU-A channel 3 from May to July 2016 in an AMSU-A all-sky experiment

retrieval, see section A.4 for details) and skewed the cloud detection in the clear-sky-through-all-sky experiments leading to significant degradations to short-range temperature forecasts. To correct this, the bias predictors for channels 3 and 4 were set to use just a constant and scan angle correction (the same as in the clear-sky system) and Fig. 30 shows that this resulted in significantly improved short-range lower tropospheric temperature forecasts as measured by improved fits between the short-range forecasts and lower peaking ATMS temperature sounding channels.

A.5.2 VarBC spin up

In the early AMSU-A all-sky experiments the variational bias correction coefficients were cold-started so that they would spin up from zero and settle into a natural equilibrium. The first problem with this approach was the sheer amount of time it took for the coefficients to reach an equilibrium. Usually research experiments are run for two periods of three months each. This is a compromise between coping with limited resources for testing and obtaining a large enough sample to attain statistical significance in the forecast scores (Geer, 2016). In the experiments where the AMSU-A all-sky bias coefficients were cold-started they took two months to reach an equilibrium and the results in the spin-up period were significantly worse than in the period once the biases had spun up. This left only one month in each period for valid verification.

The second problem with this approach was that for some channels and some predictors the bias coefficients spun up to significantly different values in the all-sky system to the clear-sky system. For some cloud affected channels this could be understood given different biases in radiative transfer models in cloudy and scattering regimes. However, the worst affected channels were the ones that peak in the stratosphere which rules out any cloud effects. For example, see Fig. 31 which shows a cubic shape in the difference between the applied bias correction for Aqua AMSU-A channels 9 to 13 across the scan. This was caused by the coefficient values for the cubic and linear terms of the polynomial scan bias correction spinning up to opposite values. The reason for this is not entirely understood but it could be related to the issues raised in sections A.6 and A.5.1.

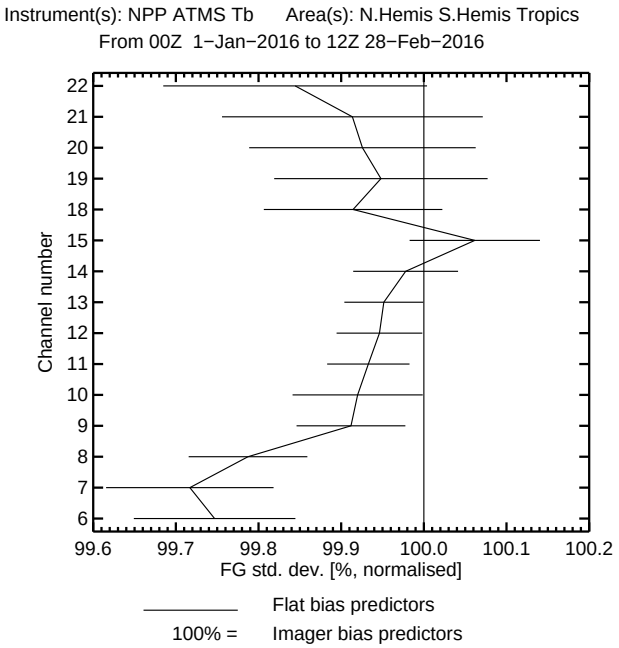

Figure 30: Change in global standard deviation of first guess departures for ATMS for an AMSU-A all-sky experiment using flat bias predictors (just constant and scan correction terms) versus an experiment using the imager bias predictors (constant, scan correction plus skin temperature and total column water vapour predictors)

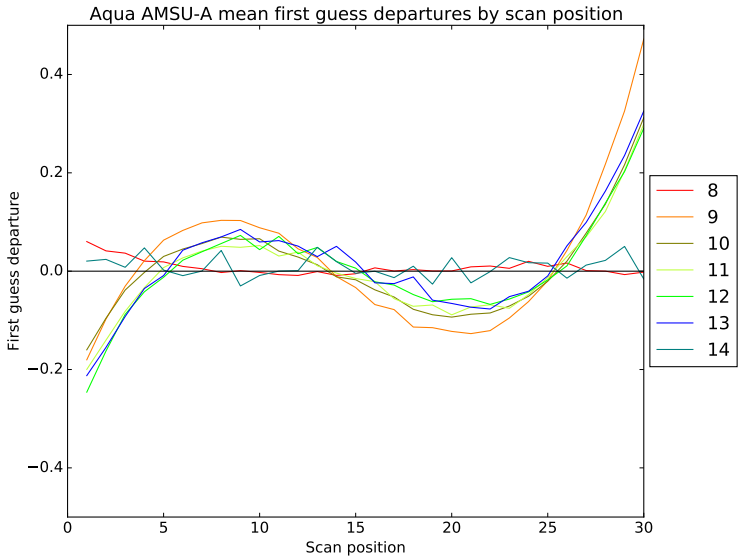

Figure 31: Difference in applied bias correction for Aqua AMSU-A channels 8-14 by scan position between all-sky and clear-sky experiments when VarBC is spun up separately in the two systems

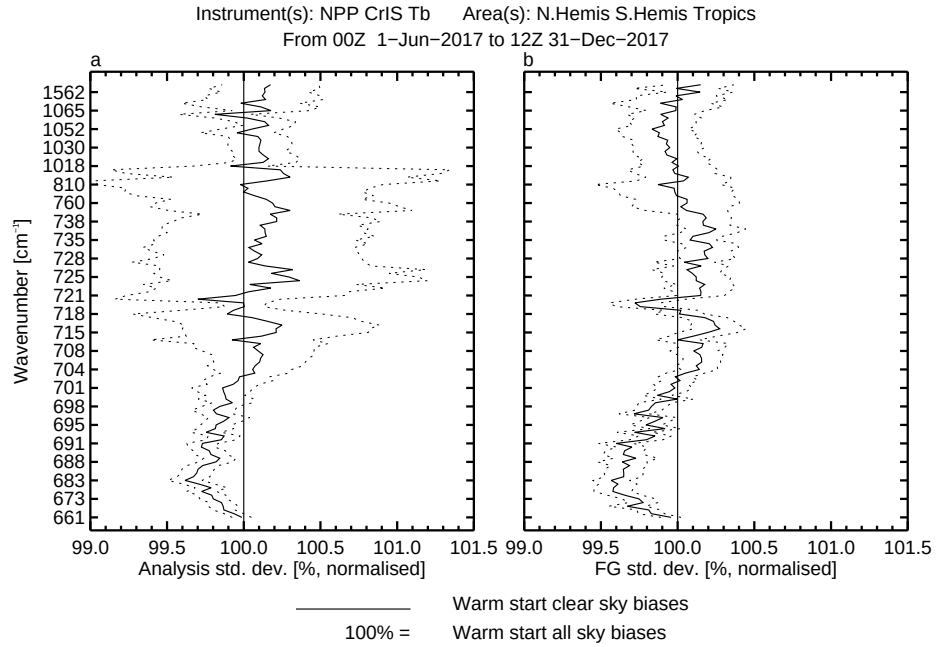

Figure 32: Change in global standard deviation of first guess departures for CrIS when warm-starting the AMSU-A all-sky bias coefficients from the clear-sky bias coefficients versus the previously spun-up all-sky bias coefficients

The workaround to both these issues is to warm start the all-sky bias coefficients using the clear-sky bias coefficients as a starting point. There is then no spin-up period and the all-sky bias coefficients remain stable over the entire experiment period of three months. Figure 32 shows that warm-starting the bias coefficients from the clear-sky values significantly improves the first guess fits to CrIS temperature sounding channels, particularly those peaking in the upper troposphere and lower stratosphere, indicating improved short-range temperature forecasts in these parts of the atmosphere.

A.6 Unexpected radiative transfer differences for stratospheric channels

During the analysis of differences between the clear-sky and clear-sky through all-sky configurations it was found that there were some unexpectedly large differences between the brightness temperatures from the clear-sky and all-sky radiative transfer models for stratospheric channels where any cloud effects should be minimal, see Fig. 33.

The reason for these differences are not fully understood but could be due to the different ways that traditional clear-sky RTTOV and all-sky RTTOV-SCATT treat levels and layers. In RTTOV the calculation uses each level as a layer average whereas in RTTOV-SCATT there are additional half-levels which are used as layer averages. The model levels in the stratosphere are further apart than in the troposphere which means this discrepancy could have a larger effect for channels sensitive in the stratosphere.

For consistency between the two systems the clear-sky radiative transfer model was used for the stratospheric channels in all all-sky experiments.

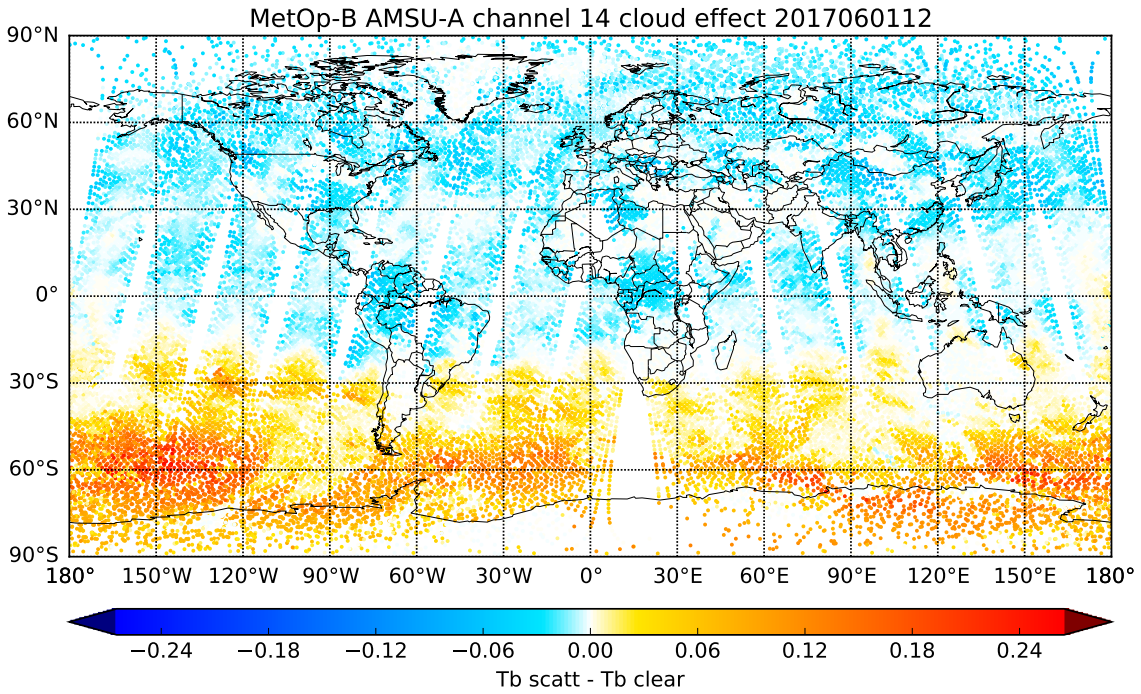

Figure 33: Difference between all-sky and clear-sky model equivalents in observation space for MetOp-B AMSU-A channel 14 data between 09UTC and 21UTC on 1st June 2017

References

Anderson, E., Järvinen, H., 1999. Variational quality control. Quarterly Journal of the Royal Meteorological Society 125 (554), 697–722.
URL https://rmets.onlinelibrary.wiley.com/doi/abs/10.1002/qj.49712555416

Auligné, T., McNally, A. P., Dee, D. P., 2007. Adaptive bias correction for satellite data in a numerical weather prediction system. Quarterly Journal of the Royal Meteorological Society 133 (624), 631–642.
URL https://rmets.onlinelibrary.wiley.com/doi/abs/10.1002/qj.56

Baordo, F., Geer, A. J., 2016. Assimilation of SSMIS humidity-sounding channels in all-sky conditions over land using a dynamic emissivity retrieval. Quarterly Journal of the Royal Meteorological Society 142 (700), 2854–2866.
URL http://dx.doi.org/10.1002/qj.2873

Bennartz, R., Thoss, A., Dybbroe, A., Michelson, D. B., 2002. Precipitation analysis using the advanced microwave sounding unit in support of nowcasting applications. Meteorological Applications 9 (2), 177–189.
URL https://rmets.onlinelibrary.wiley.com/doi/abs/10.1017/S1350482702002037

Bormann, N., 2016. Slant path radiative transfer for the assimilation of sounder radiances. ECMWF

Technical Memorandum 782.
URL https://www.ecmwf.int/node/16482

Bormann, N., Geer, A. J., Bauer, P., 2011. Estimates of observation-error characteristics in clear and cloudy regions for microwave imager radiances from numerical weather prediction. Quarterly Journal of the Royal Meteorological Society 137 (661), 2014–2023.
URL https://rmets.onlinelibrary.wiley.com/doi/abs/10.1002/qj.833

Bormann, N., Lupu, C., Geer, A. J., Lawrence, H., Weston, P., English, S., 2017. Assessment of the forecast impact of suface-sensitive microwave radiances over land and sea-ice. ECMWF Technical Memorandum 804.
URL https://www.ecmwf.int/node/17674

Dee, D., 2004. Variational bias correction of radiance data in the ECMWF system. In: ECMWF Workshop on Assimilation of high spectral resolution sounders in NWP, 28 June - 1 July 2004. ECMWF, ECMWF, Shinfield Park, Reading, pp. 97–112.
URL https://www.ecmwf.int/node/8930

Desroziers, G., Berre, L., Chapnik, B., Poli, P., 2005. Diagnosis of observation, background and analysis-error statistics in observation space. Quarterly Journal of the Royal Meteorological Society 131 (613), 3385–3396.
URL https://rmets.onlinelibrary.wiley.com/doi/abs/10.1256/qj.05.108

Ebert, E. E., Janowiak, J. E., Kidd, C., 2007. Comparison of near-real-time precipitation estimates from satellite observations and numerical models. Bulletin of the American Meteorological Society 88 (1), 47–64.
URL https://doi.org/10.1175/BAMS-88-1-47

Eyre, J. R., 2016. Observation bias correction schemes in data assimilation systems: a theoretical study of some of their properties. Quarterly Journal of the Royal Meteorological Society 142 (699), 2284–2291.
URL https://rmets.onlinelibrary.wiley.com/doi/abs/10.1002/qj.2819

Geer, A., Baordo, F., 2014. Improved scattering radiative transfer for frozen hydrometeors at microwave frequencies. Atmos. Meas. Tech. 7.

Geer, A., Baordo, F., Bormann, N., English, S., 2014. All-sky assimilation of microwave humidity sounders. Technical Memorandum 741.

Geer, A., Bauer, P., English, S., 2012. Assimilating AMSU-A temperature sounding channels in the presence of cloud and precipitation. Published simultaneously as ECMWF Technical Memoranda 670 and ECMWF/EUMETSAT Fellowship Programme Research Report No.24.

Geer, A. J., 2016. Significance of changes in medium-range forecast scores. Tellus A: Dynamic Meteorology and Oceanography 68 (1), 30229.
URL https://doi.org/10.3402/tellusa.v68.30229

Geer, A. J., 2019. Correlated observation error models for assimilating all-sky infrared radiances. Atmospheric Measurement Techniques 12 (7), 3629–3657.
URL https://www.atmos-meas-tech.net/12/3629/2019/

Geer, A. J., Baordo, F., Bormann, N., Chambon, P., English, S. J., Kazumori, M., Lawrence, H., Lean, P., Lonitz, K., Lupu, C., 2017. The growing impact of satellite observations sensitive to humidity, cloud and precipitation. Quarterly Journal of the Royal Meteorological Society 143 (709), 3189–3206.
URL https://rmets.onlinelibrary.wiley.com/doi/abs/10.1002/qj.3172

Geer, A. J., Bauer, P., 2010. Enhanced use of all-sky microwave observations sensitive to water vapour, cloud and precipitation. ECMWF Technical Memoranda 620, 41, also published as EUMETSAT/ECMWF RR20.
URL https://www.ecmwf.int/node/9518

Geer, A. J., Bauer, P., 2011. Observation errors in all-sky data assimilation. Quarterly Journal of the Royal Meteorological Society 137 (661), 2024–2037.
URL https://rmets.onlinelibrary.wiley.com/doi/abs/10.1002/qj.830

Geer, A. J., Bauer, P., Lopez, P., 2007. Lessons learnt from the 1D+4D-Var assimilation of rain and cloud affected SSM/I observations at ECMWF. ECMWF Technical Memoranda 535, 49, also released as EUMETSAT/ECMWF Fellowship Programme Research Report No. 17.
URL https://www.ecmwf.int/node/9510

Grody, N., Zhao, J., Ferraro, R., Weng, F., Boers, R., 2001. Determination of precipitable water and cloud liquid water over oceans from the NOAA 15 advanced microwave sounding unit. Journal of Geophysical Research: Atmospheres 106 (D3), 2943–2953.
URL https://agupubs.onlinelibrary.wiley.com/doi/abs/10.1029/2000JD900616

Han, W., Bormann, N., 2016. Constrained adaptive bias correction for satellite radiance assimilation in the ECMWF 4D-Var system. Technical Memorandum 783.

Karbou, F., Gérard, E., Rabier, F., 2006. Microwave land emissivity and skin temperature for AMSU-A and -B assimilation over land. Quarterly Journal of the Royal Meteorological Society 132 (620), 2333–2355.
URL http://dx.doi.org/10.1256/qj.05.216

Lawrence, H., Bormann, N., Geer, A., English, S., 2015. An evaluation of FY-3C MWHS-2 at ECMWF. EUMETSAT/ECMWF Fellowship Programme Research Report No.37.

Liu, Q., Weng, F., English, S. J., 2011. An improved fast microwave water emissivity model. IEEE Transactions on Geoscience and Remote Sensing 49 (4), 1238–1250.

Lonitz, K., Geer, A. J., 2015. New screening of cold-air outbreak regions used in 4D-Var all-sky assimilation. EUMETSAT/ECMWF Fellowship Programme Research Report No.35.

Migliorini, S., Candy, B., 2019. All-sky satellite data assimilation of microwave temperature sounding channels at the Met Office. Quarterly Journal of the Royal Meteorological Society 145 (719), 867–883.
URL https://rmets.onlinelibrary.wiley.com/doi/abs/10.1002/qj.3470

Peubey, C., McNally, A., 2009. Characterization of the impact of geostationary clear-sky radiances on wind analyses in a 4D-Var context. Quarterly Journal of the Royal Meteorological Society 135 (644), 1863–1876.
URL https://rmets.onlinelibrary.wiley.com/doi/abs/10.1002/qj.500

Saunders, R., Hocking, J., Turner, E., Rayer, P., Rundle, D., Brunel, P., Vidot, J., Roquet, P., Matricardi, M., Geer, A., Bormann, N., Lupu, C., 2018. An update on the RTTOV fast radiative transfer model (currently at version 12). Geoscientific Model Development 11 (7), 2717–2737.
URL https://www.geosci-model-dev.net/11/2717/2018/

Trigo, I., Boussetta, S., Viterbo, P., Balsamo, G., 2015. Comparison of model land skin temperature with remotely sensed estimates and assessment of surface-atmosphere coupling. ECMWF Technical Memorandum 774.
URL https://www.ecmwf.int/node/15318

Weston, P., Bormann, N., Geer, A., Lawrence, H., 2017. Harmonisation of the usage of microwave sounder data over land, coasts, sea ice and snow: First year report. EUMETSAT/ECMWF Fellowship Programme Research Report No.45.

Zhu, Y., Liu, E., Mahajan, R., Thomas, C., Groff, D., Van Delst, P., Collard, A., Kleist, D., Treadon, R., Derber, J. C., 2016. All-sky microwave radiance assimilation in NCEPs GSI analysis system. Monthly Weather Review 144 (12), 4709–4735.
URL https://doi.org/10.1175/MWR-D-15-0445.1